

UC Merced

UC Merced Electronic Theses and Dissertations

Title

Alterations of Soil Physical and Biogeochemical Properties Induced by Low Intensity Fire

Permalink

<https://escholarship.org/uc/item/2cp3q02m>

Author

Jian, Mathew

Publication Date

2017

Peer reviewed|Thesis/dissertation

UNIVERSITY OF CALIFORNIA, MERCED

Alterations of Soil Physical and Biogeochemical Properties Induced by Low Intensity Fire

A thesis submitted in partial satisfaction of the requirements for the degree
Master of Science

in

Environmental Systems

by

Mathew Jian

Committee in charge:

Teamrat A. Ghezzehei

Asmeret Asefaw Berhe

Thomas C. Harmon

Markus Berli

2017

©

Mathew Jian, 2017

All rights reserved

The Thesis of Mathew Jian is approved, and is acceptable in quality and form for publication on microfilm and electronically:

Teamrat A. Ghezzehei

Asmeret Asefaw Berhe

Thomas C. Harmon

Markus Berli

University of California, Merced

2017

Table of Content

List of Tables	6
List of Figures.....	7
Acknowledgements	9
Abstract.....	10
Chapter 1 Introduction.....	12
1.1 Background	12
1.2 Research Objectives.....	15
Chapter 2 Micromechanics of soil structural degradation during low intensity burns	17
2.1 Introduction.....	18
2.2 Methods	20
2.2.1 Soil Collection.....	20
2.2.2 Micromechanical Experiments.....	21
2.2.2.1 Heating Experiment.....	21
2.2.2.2 Soil Aggregate Tensile Strength.....	23
2.2.3 Predicting Deformation on Aggregate During Heating Experiment.....	24
2.2.3.1 Predicting viscous deformation	25
2.2.3.2 Predicting elastic deformation	28
2.3 Results	28
2.4 Discussion	32
2.4.1 Micromechanical experiment and modeling of aggregate degradation	32
2.4.2 Implications of Prescribed Burns for Ecosystem Processes.....	35
2.5 Conclusion	37
Chapter 3 Mechanism of exposing physically protected soil organic carbon to decomposition by breakdown of soil aggregates during low intensity burns.....	38
3.1 Introduction.....	39
3.2 Methods	42
3.2.1 Soil Collection.....	42
3.2.2 Gravimetric Water Content of Soil Aggregates at Field Capacity	43
3.2.3 Dissolved organic carbon leaching experiment	43
3.2.3.1 Laboratory Heating Treatments.....	43
3.2.3.2 Soil Leachate Collection and Analysis.....	44
3.2.4 CO ₂ Respiration Rate	45
3.2.4.1 Laboratory Heating Treatments.....	45
3.2.4.2 CO ₂ Measurements	46
3.2.4.3 Soil Organic Carbon Mineralization Rate	46
3.2.5 Statistical analysis	47
3.3 Results.....	48

3.3.1	Dissolved Organic Carbon concentration of leachate	48
3.3.2	Specific UV Absorbance of leachate	49
3.3.3	Average molecular size of dissolved organic carbon in leachate.....	51
3.3.4	CO ₂ measurements	52
3.4	Discussion	60
3.4.1	Dissolved organic carbon analysis in soil leachate	60
3.4.2	CO ₂ measurements in forest soil	62
3.4.3	CO ₂ measurements in shrubland soil.....	64
3.5	Conclusion	67
Chapter 4 Summary and Conclusion		68
References		72
Appendix A Measuring soil moisture evaporation rate during heating treatments.		81
Appendix B Energy partitioning calculation.....		83
B.1	Calculating E_{H_2O} and E_{vap}	83
B.2	Calculating E_{soil}	84
B.3	Calculating E_{blk}	85
B.4	Results and discussion of energy partitioning calculation	86
Appendix C Organic carbon content of large soil aggregates		87

List of Tables

Table 2-1 Characterization of studied soil (mean \pm standard deviation, where n = 4 for forest soil textural data and n = 3 for other data). *Values previously reported by Albalasmeh et al (2013).....	20
Table 2-2 Summary table of aggregates used in heating and tensile strength experiment.....	24
Table 2-3 Summary table of model parameters used for modeling yield stress, viscosity, and shear modulus. Parameters were fitted to data previously reported by Ghezzehei and Or (2001)	26
Table 2-4 Water content of the soil aggregates at the studied matric potential (mean \pm standard error, where n = 5 for forest soil and n = 3 for shrubland soil)	27
Table 3-1 Characterization of studied soils (mean \pm standard error, where n = 3 to 5. Clay content is expressed in mean \pm standard deviation, where n = 4 for forest soil and n = 3 for shrubland soil) *Value previously reported by Albalasmeh et al (2013).....	43

List of Figures

Figure 1-1 Percentage of burned areas characterized as low severity burns in southwest United States ($P = 0.38$) (MTBS, 2017).	16
Figure 2-1 Pictures of experiments conducted. (a) Direct measurement of pneumatic pressure inside aggregate during heating experiment. (b) Direct measurement of tensile strength by pulling apart aggregates with epoxied ends until they break apart at the failure plane (c)	22
Figure 2-2 Example plots of the pneumatic gas pressure rise inside the (a) forest and (b) shrubland soil, and soil surface temperature of the (c) forest and (d) shrubland soil during heating experiment. Air-dried matric potentials for the forest and shrubland soil are -94,230 kPa and -123,603 kPa, respectively	29
Figure 2-3 Maximum internal pressure and tensile strength of (a) forest and (b) shrubland soil over multiple matric potentials. Values are averaged of between 7 and 20 replicates for the maximum pneumatic stress measurements, and between 3 and 11 replicates for the tensile strength measurements, with error bars representing standard error in the y-axis.....	30
Figure 2-4 The range of predicted viscous strain experienced by (a) forest and (b) shrubland soil due to pneumatic gas pressure increase during the heating experiment. Note the y-axis scale is not the same for both of the plots	31
Figure 2-5 The range of predicted elastic strain experienced by (a) forest and (b) shrubland soil due to pneumatic gas pressure increase during the heating experiment.....	32
Figure 3-1 Dissolved organic carbon (mg L^{-1}) in the soil leachate from unburned (UB), rapidly burned dried (DRB), slowly burned (SB) and rapidly burned (RB) soil aggregates from (a) forest soil and (b) shrubland soil. Different letters represent significantly different means as determined from Tukey's HSD Test ($P < 0.05$)	49
Figure 3-2 SUVA_{254} in the soil leachate from unburned (UB), rapidly burned dried (DRB), slowly burned (SB) and rapidly burned (RB) soil aggregates from (a) forest soil and (b) shrubland soil. Different letters represent significantly different means as determined from Tukey's HSD Test ($P < 0.05$)	50
Figure 3-3 $A_{250}:A_{365}$ in the soil leachate from unburned (UB), rapidly burned dried (DRB), slowly burned (SB), and rapidly burned (RB) soil aggregates from (a) forest soil and (b) shrubland soil. No significant differences were found between burn treatments.....	51
Figure 3-4 Cumulative $\text{CO}_2\text{-C}$ loss in $\mu\text{gC g soil}^{-1}$ for forest soil with aggregate sizes (1) 0.25-1 mm and (2) 1-2 mm. Rows (a-d) indicate UB, DRB, SB, and RB treatments, respectively.....	53
Figure 3-5 Cumulative $\text{CO}_2\text{-C}$ loss in $\mu\text{gC g soil}^{-1}$ for shrubland soil with aggregate sizes (1) 0.25-1 mm and (2) 1-2 mm. Rows (a-d) indicate UB, DRB, SB, and RB treatments, respectively.	54

- Figure 3-6 C_0 of unburned (UB), rapidly burned dried (DRB), rapidly burned (RB) and slowly burned (SB) soil aggregates from forest soil with aggregate sizes (a) 0.25 to 1 mm and (b) 1 to 2 mm, and shrubland soil with aggregate sizes (c) 0.25 to 1 mm and (d) 1 to 2 mm. Different letters represent significantly different means as determined from Tukey's HSD Test ($P < 0.05$) 55
- Figure 3-7 $C_0:C_a$ (the ratio of the biologically available carbon pool to the total carbon pool (C_a)) of unburned (UB), rapidly burned dried (DRB), rapidly burned (RB) and slowly burned (SB) soil aggregates from forest soil with aggregate sizes (a) 0.25 to 1 mm and (b) 1 to 2 mm, and shrubland soil with aggregate sizes (c) 0.25 to 1 mm and (d) 1 to 2 mm. Different letters represent significantly different means as determined from Tukey's HSD Test ($P < 0.05$) 57
- Figure 3-8 k of unburned (UB), rapidly burned dried (DRB), rapidly burned (RB) and slowly burned (SB) soil aggregates from forest soil with aggregate sizes (a) 0.25 to 1 mm and (b) 1 to 2 mm, and shrubland soil with aggregate sizes (c) 0.25 to 1 mm and (d) 1 to 2 mm. Different letters represent significantly different means as determined from Tukey's HSD Test ($P < 0.05$) 59
- Figure 3-9 Ratio of DOC:TOC vs ratio of $C_0:C_a$ for (a) forest soil and (b) shrubland soil for the two aggregate sizes, where $C_0:C_a$ represents the ratio of the biologically available carbon pool to the total carbon pool (C_a), and DOC:TOC represents the ratio of dissolved organic carbon leached to the total organic carbon..... 66

Acknowledgements

My journey through UC Merced would not have been possible without the support of many individuals around me. I would like to extend my gratitude to the following:

My advisor, Teamrat Ghezzehei, for his endless support and encouragement throughout my graduate studies. Your knowledge and passion for science have inspired me to become the best scholar I can be. I could not have asked for a better mentor.

My committee members: Asmeret Asefaw Berhe, Thomas C. Harmon, and Markus Berli for your comments, suggestions, and ideas.

Liyang Zhao, for the help provided with the TOC analyzer through the Environmental Analytical Laboratory at UC Merced.

Rose Shillito, from the Desert Research Institute, for your comments, feedback, friendship, and help in the shrubland soil collection.

Past and current members of the Ghezzehei and Berhe groups: My progression through graduate school would not have been possible without your comments, feedback, and support. Also, you guys remind me that I can still be a kid – you know, since we get our hands dirty with soil all day. I would like to give special thanks to Rebecca Abney and Fernanda Santos from the Berhe group for help in operating some of the laboratory instruments.

All the amazing and awesome friends that I met here at UC Merced. I would especially like to thank Shagun Rawat, Rafay Qureshi, and Christine Hoffman. You guys were my family away from home. Your friendship is invaluable and reminds me that graduate school can be fun! I look forward to the many mischievous adventures we will continue to have even after our graduate studies.

My brothers, Mike and Andy. Thank you guys for the great support and encouragement throughout our childhood and even to this day, and also for giving me places to crash when I am back at home.

My best friend, Iris Liu. You believe in me even through my tough times in my graduate studies. You listen to me when I need someone to talk to. Thank you for your love and support; it will forever be ingrained in my heart.

The National Science Foundation, for funding my thesis research.

Last, but not least, I would like to express my most sincere gratitude to my parents. I am grateful for your unconditional love, and I would not be where I am today if it weren't for all the sacrifices you have made.

Abstract

Alterations of Soil Physical and Biogeochemical Properties Induced by Low Intensity Fire

by

Mathew Jian

Masters of Science in Environmental Systems

University of California, Merced, 2017

Teamrat A. Ghezzehei, Chair

Soil aggregate degradation by medium and high intensity fires is often attributed to loss of soil organic matter, whereas low intensity fires are often considered benign to soil aggregate degradation because organic and inorganic binding agents are relatively stable at these low temperature burns. Because of this, there are limited studies specifically focusing on the effect of low intensity fires on soil aggregation. However, recent long-term studies have reviewed that aggregate breakdown can occur long periods of time after low intensity burns. The aggregate breakdown could not be explained by loss of soil binding agents. Previous studies have indirectly tested the hypothesis that stress exerted by rapid vaporization of soil pore water during low intensity burns could lead to aggregate breakdown in the long term. I further explore this mechanism of soil aggregate degradation in a forest sandy loam and shrubland loam soil. In this work, I (1) provide direct proof of the hypothesis by measuring the pressure inside individual moist soil aggregates burned at 175°C and (2) show that soil aggregate degradation by this mechanism can expose physically protected soil organic carbon to decomposition. The pore pressure increase in both the forest and the shrubland aggregates increased with increasing soil water content. Furthermore, tensile strength of both types of soil

aggregates decreased with increase in soil water content, suggesting that moist soil aggregates may be more susceptible to breakdown by this mechanism. Additionally, I provide a model predicting that strain on aggregates from rapidly vaporized soil water is maximized in initially wetter soil aggregates. The degradation of soil aggregates by rapidly vaporized soil pore water was observed in forest soils that experienced increase in rate of decomposition of soil organic following low intensity fires. Increase in decomposition of soil organic carbon in shrubland soil aggregates were observed for all burn treatments, and was linked to increase in dissolved organic carbon likely due to loss of cytoplasmic organic compounds from lysis of soil microbes. The results provided in this thesis suggest that low intensity burns can negatively affect soil aggregation in ways that were not studied before since low intensity burns are often considered benign to soil aggregation, and that more research should focus on low intensity fires' effects on soil aggregates as the number of these burns have been increasing over the last few decades.

Chapter 1

Introduction

1.1 Background

Fires affect natural ecosystem patterns through interactions with geomorphic processes and landforms at multiple temporal and spatial scales (Swanson, 1981). Some of the effects of fire include alteration of: soil erosion and sediment transport processes across watersheds, landform constraints on fire behavior and burn boundaries, and vegetation and soil properties. The degree of fire-induced soil property changes is largely determined by the fire severity (the degree of ecological effects of the fire), which is dependent on the fire intensity (the time-averaged energy flux of the fire) (Keeley, 2009).

The effects of medium and high intensity fires (soil surface temperature > 220°C) – which include many wildfires observed in forest ecosystems – on soils are widely recognized. These fires can lead to increased rate of soil erosion (Benavides-Solorio and MacDonald, 2001; Carroll et al., 2007), increased hydrophobicity of the subsoil (Debano, 2000), and reduction of water infiltration (Debano, 2000) and water holding capacity (Stoof et al., 2010). One soil property that is often studied post-medium and high intensity fires is soil aggregation (structure) since soil aggregation is often used as an indicator of soil health (Mataix-Solera et al., 2011). These fires often lead to loss of soil aggregation, and the major mechanisms that drive the loss of soil aggregation are loss

of soil organic matter and nutrients through volatilization (Araya et al., 2017), ash entrapment in smoke columns, leaching and erosion, quantitative and qualitative alteration of microbial communities, and degradation of aggregate stability (Mataix-Solera et al., 2011).

In contrast, there are only a limited number of studies that have focused on the effects of low intensity fires – which include natural burns in many arid/semi-arid ecosystems and controlled burns for natural resource management – on soils as they are presumed to have minor effects on landscape and ecosystem processes (DeBano et al., 1977; Mataix-Solera et al., 2011). For example, low to moderate intensity fires were shown to have no significant effect on the loss of soil C and N content (Moghaddas and Stephens, 2007). Prescribed burns have also been shown to increase soil nutrient availability and C content (Scharenbroch et al., 2012). With respect to low intensity burns on soil aggregation, and in particular, soil aggregate stability, some studies found no significant changes immediately after the burns (Mataix-Solera et al., 2002; Arcenegui et al., 2008; Zavala et al., 2010; Jordán et al., 2011), and some observed an increase in aggregate stability due to addition of organic matter and/or desiccation-induced hardening of inorganic cements (Guerrero et al., 2001; Mataix-Solera et al., 2002; Mataix-Solera and Doerr, 2004).

However, recent long-term studies on the effect of low intensity fires on soil aggregation reveal that substantial loss of aggregate stability can occur months to years after the burn, even though there were no substantial losses in soil organic matter. The degradation of soil aggregation can lead to reduced infiltration and loss of soil porosity (Bronick and Lal, 2005). One study (Úbeda and Bernia, 2005) on forest soil aggregates in

northeastern Spain found that low intensity burns increased soil aggregate stability immediately after the burn. However, there was no mechanistic explanation for the decrease in aggregate stability observed eight months later. The observed decrease in aggregate stability remained even two years after the burn. Similar observations were made after a controlled, low severity burn was conducted in a shrubland in the eastern Great Basin in Nevada (Chief et al., 2012; Kavouras et al., 2012). The soil aggregates degraded from blocky structure to structureless 13 months after the burn.

The preceding observations suggest that the mechanisms of soil aggregate degradation under low intensity burns are characteristically different from medium and high intensity fires in at least two major ways: (1) degradation of soil aggregates from low intensity fire does not involve loss in soil organic matter content, and (2) the effects of low intensity fire take effect after a considerable amount of time. The latter observation implies that the effect of low intensity burns on soil aggregation is likely to be overlooked in assessments that focus only on the immediate aftereffects. This is of concern as low severity burns account for approximately half of the combined wildfire and controlled burn areas reported in the United States between 1984 and 2014 (MTBS, 2017), roughly 6.5×10^7 acres of land.

One mechanism of soil aggregate degradation under low intensity fire was proposed by Albalasmeh et al. (2013). The authors proposed that stress exerted by expansion of entrapped air or rapid vaporization of soil pore water during low intensity burns could lead to aggregate breakdown in a process similar to air slaking from initially dry soil aggregates submerged in water (Hillel, 1998). Albalasmeh et al. (2013) was the

first study to suggest and indirectly investigate this mechanism of soil aggregate degradation during low intensity burns (Urbanek, 2013).

1.2 Research Objectives

The overall objective of this thesis was to further explore the effects of rapid vaporization of soil pore water from low intensity fires on the stability of soil aggregates. In addition to studying this mechanism, I also studied how such a mechanism can lead to changes in decomposition of soil organic carbon. The motivation for this study was to address the need for more research on the effects of low intensity fires on soil aggregation. Furthermore, the percentage of burned areas that are characterized as low severity burns in the southwestern United States have increased over the past few decades and is projected to increase (MTBS, 2017) (Figure 1-1). The specific objectives of this research are as follows:

1. To determine the driver and mechanism of soil aggregate degradation from rapid vaporization of soil pore water during low intensity burns;
2. To evaluate the effects of degradation of soil aggregation by this mechanism on losses of soil organic carbon.

The above research objectives are presented as individual chapters within this thesis. Chapter 2 will address the first research objective, focusing heavily on the physical process of soil aggregate degradation. Chapter 3 will address the effects of soil aggregate degradation on soil biogeochemical processes, especially on decomposition of

soil organic carbon. Finally, Chapter 4 serves as an overall summary of the thesis, conclusions, and recommendations for future studies.

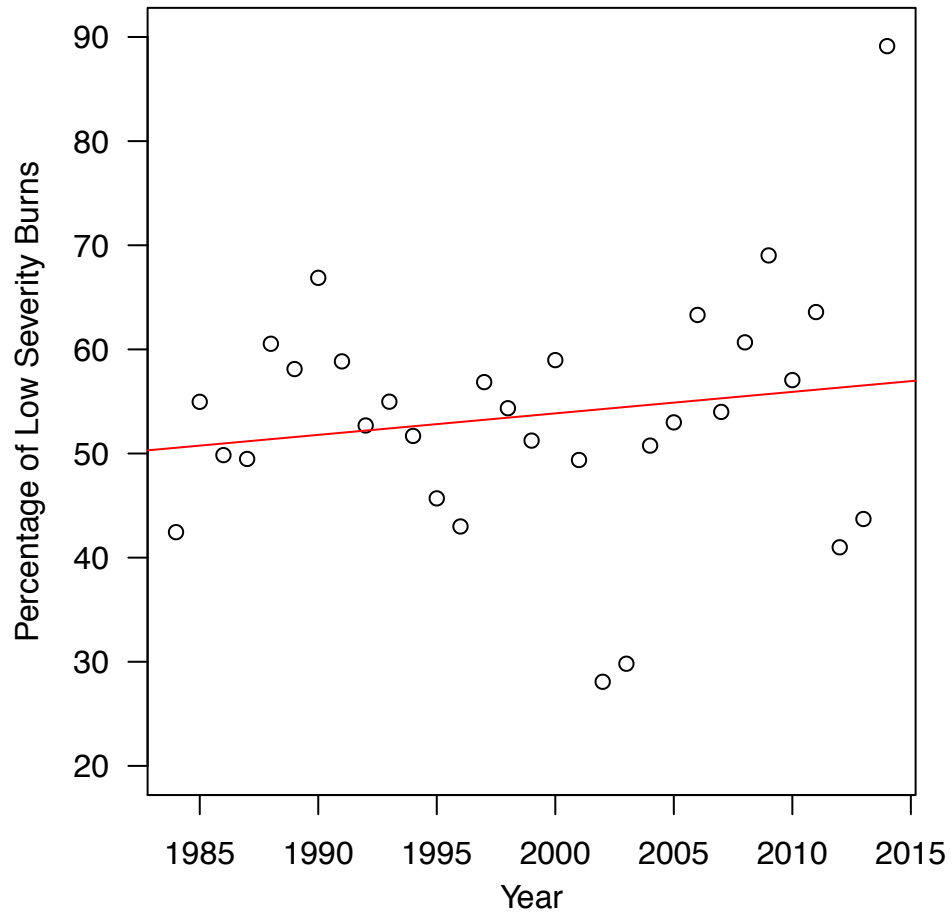


Figure 1-1 Percentage of burned areas characterized as low severity burns in southwest United States ($P = 0.38$) (MTBS, 2017).

Chapter 2

Micromechanics of soil structural degradation during low intensity burns

Abstract

Soil aggregate degradation by high intensity fires is often attributed to loss of soil organic matter. Therefore, controlled burns are generally managed to be low in intensity. This is typically done by conducting controlled burns on wet soil conditions. However, recent studies suggest that conducting controlled burns in moist soil conditions may accelerate soil aggregate degradation. Here we show that in low intensity burns, rapidly vaporized soil pore water can cause pneumatic gas pressure to increase within the soil aggregate, which can cause strain on the soil aggregates that can produce microscopic breakdowns, especially for initially moist soil aggregates. Furthermore, the tensile strength of soil aggregates are shown to be orders of magnitude lower for moist soil aggregates, which indicate that moist soil aggregates may be more susceptible to breakdown by this mechanism than dry aggregates. Our results demonstrate that rapidly vaporized soil pore water during a controlled, low intensity burn can lead to soil aggregate degradation. This is especially important as this phenomenon is often overlooked and can have implications on many ecosystem processes. Although our results indicate that it is advantageous to

conduct controlled burns during drier soil conditions, it is important to weigh in the implications of dry soil conditions and burn severity.

2.1 Introduction

The extent of fire-induced ecosystem and geomorphic alterations depend on the intensity (time-averaged energy flux) and severity (degree of ecological effects) of fire (Keeley, 2009). In soils, fire severity is expressed in terms of peak temperature and duration of elevated temperature in the soil profile (Mataix-Solera et al., 2011). Medium-to-high-intensity fires, with surface soil temperature exceeding 220° C, cause significant intensification of runoff and erosion, and have been the subject of numerous investigations worldwide (DeBano et al., 1977; Certini, 2005; Carroll et al., 2007; Knicker, 2007). This is often attributed to the loss and volatilization of soil organic matter at such temperatures (Mataix-Solera et al., 2011). In contrast, low intensity burns are generally presumed to have minor adverse effects on soil processes (DeBano et al., 1977; DeBano, 2000; Mataix-Solera et al., 2011), but only limited studies were directed at this topic. While most of these investigations reported no significant change of soil structure immediately after low-intensity burns (Mataix-Solera et al., 2002; O'Dea, 2007; Arcenegui et al., 2008; Jordán et al., 2011), a few found slight-to-moderate increase in aggregate stability that was attributed to addition of organic matter and/or desiccation-induced hardening of organic and inorganic cements (Mataix-Solera et al., 2002; García-Corona et al., 2004; Úbeda and Bernia, 2005). However, long-term monitoring of soil structure following low intensity fires in Northeastern Spain (Úbeda and Bernia, 2005)

and Great Basin region of Nevada (Chief et al., 2012; Kavouras et al., 2012) revealed significant deterioration of soil aggregate stability eight to thirteen months after the burns.

Previously, Albalasmeh et al (2013) hypothesized a mechanism that explains this delayed onset of soil aggregate deterioration. When the temperature is raised rapidly to above boiling point, pore water is vaporized causing the pore pressure to rise momentarily. If the peak pressure approaches or exceeds the tensile strength of the cements that bond soil particles together, the overall stability of the aggregates would be compromised. Albalasmeh et al (2013) indirectly tested the hypothesis by showing that the water stability of aggregates rapidly heated to 175° C is lower than aggregates slowly heated to the same degree. The latter case was assumed to be less damaging because the vapor has sufficient time to escape without elevating the internal pressure to damaging levels. Albalasmeh et al (2013) was the first study to suggest and indirectly test this mechanism of soil aggregate degradation during low intensity burns (Urbanek, 2013). Here we provide a direct proof of the hypothesis by measuring the pressure inside individually burned soil aggregates. We show that the pressure inside moist aggregates can be elevated to 3.25 kPa while the pressure in air-dry aggregates remains in equilibrium with the atmosphere. The pore pressure measured within the soil aggregates during a low intensity burn is comparable to the tensile strength of the aggregates, which suggest that the rapidly vaporized soil moisture can potentially cause substantial weakening of the aggregates. These types of burns affect half of the combined wildfire and prescribed burn areas reported in the U.S. between 1984 and 2016 (Eidenshink et al.,

2007; MTBS, 2017). Therefore, soil aggregate degradation by the proposed mechanism during low intensity burns may be relevant for many burned areas.

2.2 Methods

2.2.1 Soil Collection

Soils were collected from two distinct ecosystems that experience low severity fires in the western United States. The first soil collected was a sandy loam from an undisturbed pine forest in Mariposa County, United States. The second soil was a loam collected from an unburned shrubland (adjacent to the burn boundary of the Carpenter 1 Fire) in Clark County, United States. In the subsequent sections of this paper, these soils will be referred to as forest and shrubland soils, respectively. Soil samples were collected from 0-10 cm depth then air-dried. For the forest soil, large aggregates of masses between 1.5 and 4.0 grams were separated out by hand. For the shrubland soil, large aggregates between 1.3 and 5.3 grams were separated by hand. Basic characteristics of the soils are provided in Table 2-1.

Table 2-1 Characterization of studied soil (mean \pm standard deviation, where $n = 4$ for forest soil textural data and $n = 3$ for other data). *Values previously reported by Albalasmeh et al (2013).

Soil	Texture	Sand (%)	Silt (%)	Clay (%)	Organic carbon (%)
Forest	Sandy loam	69.20 \pm 8.76*	19.25 \pm 3.88*	11.55 \pm 4.90*	4.09 \pm 0.88
Shrubland	Loam	37.86 \pm 1.02	41.09 \pm 1.52	21.05 \pm 0.86	0.36 \pm 0.02

2.2.2 Micromechanical Experiments

We conducted two different experiments that allow direct testing of the hypothesis that the pore pressure of moist aggregates subjected to low-intensity burns is elevated to a degree that can deteriorate the stability of the aggregate bonds. In the first experiment, we carried out a heating treatment to directly measure the pneumatic pore pressure rise within the moist soil aggregates during a low-intensity burn. In the second experiment, we measured the soil aggregate tensile strength and to compare the strength of the soils to the maximum pneumatic pressure observed within the aggregates during the heating experiment.

2.2.2.1 Heating Experiment

Five matric potentials for each soil type were chosen as the initial matric potentials of the soil aggregates before aggregates were heated: -6 kPa, -10 kPa, -30 Kpa, -100 kPa, and air-dried conditions (-94,230 kPa for the forest soil and -123,603 kPa for the shrubland soil). The latter matric potentials corresponded to air-dried soil conditions, which were determined by dry sieving 5 g aggregates to the size of 0.5-2 mm and taking triplicate measurements in a dewpoint potentiometer (Decagon Devices WP4).

Prior to the heating experiment to measure the internal pressure elevation, soil aggregates were wetted to the selected matric potentials by placing them on porous plates inside a pressure plate apparatus (Soilmoisture Equipment Corp pressure plate extractor). The forest aggregates were then gradually wetted by capillary action from a thin film of water on top of the porous plates. The shrubland aggregates were lightly sprayed by a

fine mist of water prior to being gradually wetted by capillary action. The aggregates were equilibrated at the desired matric potential level for 24 hours.

To measure the pressure elevation of heated aggregates, an aggregate pressure sensor was developed (Figure 2-1). The sensor involves a pressure transducer (Honeywell sensor number 26PCCFA6G) connected to a BD 0.45mm x 10mm hypodermic needle. To measure the pressure elevation of air dried soil aggregates during the heating experiment, the hypodermic needles were inserted into a subset of -100 kPa matric potential soil aggregates and then air dried for 48 hours before being connected to the pressure transducer.

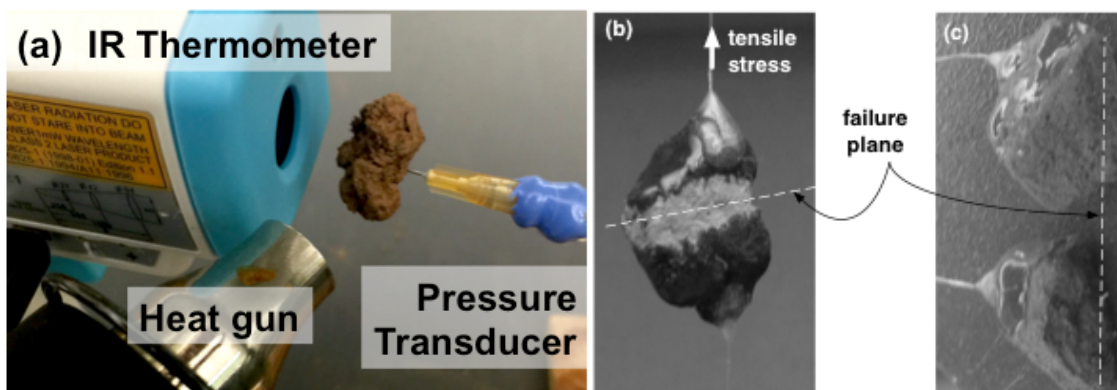


Figure 2-1 Pictures of experiments conducted. **(a)** Direct measurement of pneumatic pressure inside aggregate during heating experiment. **(b)** Direct measurement of tensile strength by pulling apart aggregates with epoxied ends until they break apart at the failure plane **(c)**.

The aggregates were heated with a heat gun (Milwaukee heat gun model 1400) for 15 minutes at temperatures around 175°C that corresponds to typical temperatures found in low intensity burns. The heat gun was connected to a variable autotransformer (POWERSTAT Type 2PF136) to control the temperature of heat flowing out of the heat

gun nozzle. During the heating process, the surface temperature of the soil aggregate was continuously recorded with an infrared thermometer (Omega infrared thermometer OS1327D). Internal pressure elevation inside of the aggregates over the course of the heating experiment was continuously logged by a data logger (Keithley 2700 Multimeter/Data Acquisition System).

2.2.2.2 Soil Aggregate Tensile Strength

To measure the tensile strength of the soil aggregates, a separate set of soil aggregates were coated with epoxy while leaving a narrow, uncoated band that pre-defined the tensile shear plane. Thin strings were connected to both sides of the aggregates epoxy coatings (Figure 2-1b,c), and the epoxy was allowed to dry for 72 hours. Afterwards, a micrometer caliper was used to measure the length and width of the pre-defined tensile shear plane, and the cross sectional area of the tensile shear plane was approximated as an ellipse.

The tensile strength of the aggregates was measured at five matric potentials: -10 kPa, -30 kPa, -100 kPa, -2200 kPa, and air-dried conditions (-94,230 kPa for the forest soil and -123,603 kPa for the shrubland soil). Aggregates were equilibrated to -10 kPa, -30 kPa, and -100 kPa in the same fashion as the aggregates used in the heating experiment with the pressure plate apparatus. To equilibrate the aggregates to -2200 kPa, a subset of pre-equilibrated -100 kPa aggregates was placed in a desiccator filled with 0.5 M KCl solution (water potential = -2200 kPa) for 7 days.

After the soil aggregates were equilibrated to the desired matric potential, the soil aggregates were then suspended in air. Weights were steadily added to the bottom to

apply tensile stress until the aggregates ruptured along the pre-defined tensile shear plane (Figure 2-1). The tensile stress was then calculated with the mass required to rupture the aggregates over the area of the pre-defined tensile shear plane. A summary of the soil aggregates used in these experiments is provided in Table 2-2.

Table 2-2 Summary table of aggregates used in heating and tensile strength experiment

Soil	Heating experiment			Tensile strength experiment	
	Matric potential (-kPa)	n	Mass range (g)	Matric potential (-kPa)	n
Forest	6	18	1.49 - 4.01	10	3
	10	20	1.52 - 3.97	30	11
	30	16	1.65 - 4.01	100	4
	100	13	1.54 - 3.86	2200	3
	94230	13	1.79 - 3.99	94230	3
Shrubland	6	11	1.28 - 4.89	10	6
	10	13	1.72 - 4.08	30	5
	30	16	1.34 - 5.24	100	5
	100	17	1.62 - 4.10	2200	6
	123603	7	1.32 - 4.32	123603	5

2.2.3 Predicting Deformation on Aggregate During Heating Experiment

While the experiments described in the preceding sections help to describe how maximum pore pressure rise and aggregate tensile strength are related to the initial moisture level of the soil aggregates, these experiments have their limitations. First, the aggregate tensile strength measurements only show the maximum stress required to fully break the soil aggregates. The soil aggregates do not fully break during the course of a low intensity burn, and the pore pressure rise within the aggregate is only expected to disrupt the microscopic bonds between soil particles. And second, the soil aggregate dries

during the course of the heating experiment; thus the tensile strength of the soil is expected to increase as the soil aggregate dries during the heating experiment. Here, we address the limitations to the experiments with a model for the viscous and elastic deformation of the soil aggregates during a low intensity burn, in which the soil physical properties change as a function of moisture content and time. The goal of this model is to provide a semi-quantitative indication of the degree of pre-failure deformation caused by the pore pressure rise within the soil aggregates during a low intensity burn.

2.2.3.1 *Predicting viscous deformation*

The soil aggregates are assumed to behave as a Bingham visco-plastic material, where the viscous strain rate is given as

$$\frac{d\gamma}{dt} = \begin{cases} 0 & \tau < \tau_0 \\ (\tau - \tau_0) / \eta & \tau \geq \tau_0 \end{cases} \quad (\text{Eq. 2.1})$$

where γ is the strain, τ is the stress applied to the Bingham visco-plastic material, τ_0 is the yield stress, and η is the plastic viscosity. Here, the stress applied to the soil aggregates is the internal pore pressure measured during the duration of the heating experiment. The yield stress of the soil aggregates was modeled as a power function of the soil gravimetric water content

$$\tau_0 = \tau_a \omega^{-\tau_b} \quad (\text{Eq. 2.2})$$

where ω is the gravimetric water content, and τ_a and τ_b are fitting parameters that were fitted to Millville silt loam, Fraternidad clay, and kaolinite reported in Ghezzehei and Or (2001). The viscosity of the soil aggregates were also modeled as a power function of the soil gravimetric water content

$$\eta = \eta_a \omega^{-\eta_b} \quad (\text{Eq. 2.3})$$

where η_a and η_b are fitting parameters that were fitted to Millville silt loam, Fraternidad clay, and kaolinite reported in Ghezzehei and Or (2001). The parameters used to model yield stress and viscosity is summarized in Table 2-3.

Table 2-3 Summary table of model parameters used for modeling yield stress, viscosity, and shear modulus. Parameters were fitted to data previously reported by Ghezzehei and Or (2001)

Model soil	Texture	τ_a (kPa g _w g _s ⁻¹)	τ_b	η_a (kPa g _w s ⁻¹ g _s ⁻¹)	η_b	G_a (kPa g _w g _s ⁻¹)	G_b
Millville	Silt loam	4.39 x 10 ⁻⁵	8.19	5.70 x 10 ⁻³	7.43	1.52 x 10 ⁻³	8.44
Fraternidad	Clay	4.81 x 10 ⁻¹	3.75	3.14 x 10 ⁻¹	5.61	1.95 x 10 ⁰	6.63
Kaolinite	Clay	2.02 x 10 ⁻¹	3.78	1.86 x 10 ⁰	5.73	1.24 x 10 ¹	4.96

To model the water content during the heating experiment, the initial gravimetric water contents of the soil aggregates before the heating treatment were calculated. A subset of soil aggregates was separated by hand. The gravimetric water contents of the soil aggregates at the selected matric potentials were determined by wetting the soil aggregates to the selected matric potentials (-6 kPa, -10 kPa, -30 kPa, and -100 kPa) by placing them on porous plates inside a pressure plate apparatus. The forest aggregates were then gradually wetted by capillary action from a thin film of water on top of the porous plates. The shrubland aggregates were lightly sprayed by a fine mist of water prior to being gradually wetted by capillary action. The aggregates were equilibrated at the desired matric potential levels for 24 hours. Afterwards, they were removed from the plate, and the gravimetric water contents were determined by drying the soil aggregates in an oven at 105°C for 24 hours. The gravimetric water content of air-dried soil

aggregates was also determined by drying air-dried soil aggregates in the same fashion.

The gravimetric water content of the soil aggregates is summarized in Table 2-4.

Table 2-4 Water content of the soil aggregates at the studied matric potential (mean \pm standard error, where $n = 5$ for forest soil and $n = 3$ for shrubland soil)

Soil	Matric potential (-kPa)	Water content (g_w g_s⁻¹)
Forest	6	0.413 \pm 0.009
	10	0.359 \pm 0.015
	30	0.318 \pm 0.024
	100	0.311 \pm 0.024
	94230	0.022 \pm 0.000
Shrubland	6	0.195 \pm 0.003
	10	0.180 \pm 0.008
	30	0.174 \pm 0.010
	100	0.138 \pm 0.010
	123603	0.024 \pm 0.003

The soil moisture content of the soil aggregates were modeled to decrease exponentially

$$\omega = \omega_0 e^{-kt} \quad (\text{Eq. 2.4})$$

where ω_0 is the initial gravimetric water content of the soil aggregate, and k is the first order decay constant. k ranged from $2.64 \times 10^{-3} \text{ s}^{-1}$ to $4.89 \times 10^{-3} \text{ s}^{-1}$ for the forest soil, and $4.24 \times 10^{-3} \text{ s}^{-1}$ to $6.11 \times 10^{-3} \text{ s}^{-1}$ for the shrubland soil (See Appendix A for determining k).

The viscous strain is evaluated as the summation of the strain rate at the times where the stresses applied to the soil aggregates exceed the yield stress.

2.2.3.2 Predicting elastic deformation

Under low stress, if the soil aggregates does not undergo viscous deformation it is assumed that the soil aggregates undergo elastic deformation

$$\gamma_e = \frac{\tau}{E} \quad (\text{Eq. 2.5})$$

where γ_e is the elastic deformation, and E the elastic modulus. The elastic modulus can be calculated as

$$E = 2G(1 + \nu) \quad (\text{Eq. 2.6})$$

where G is the shear modulus, and ν is the Poisson's ratio, assumed to 0.5. The shear modulus soil aggregates were also modeled as a power function of the soil gravimetric water content

$$G = G_a \omega^{-G_b} \quad (\text{Eq. 2.7})$$

where G_a and G_b are fitting parameters that were fitted to Millville silt loam, Fraternidad clay, and kaolinite reported in Ghezzehei and Or (2001). The parameters used to model the shear modulus summarized in Table 2-3.

2.3 Results

Measurements of pneumatic pore pressure inside the soil aggregates and the soil aggregate surface temperatures during the heating experiment are given in Figure 2-2. The plots for the forest and shrubland soils are plotted on the left and right, respectively. In each plot, only one curve is shown for each of the matric potentials measured. For the

forest soils, a total of 80 aggregates were heated over the five matric potentials. For the shrubland soils, a total of 64 aggregates were heated.

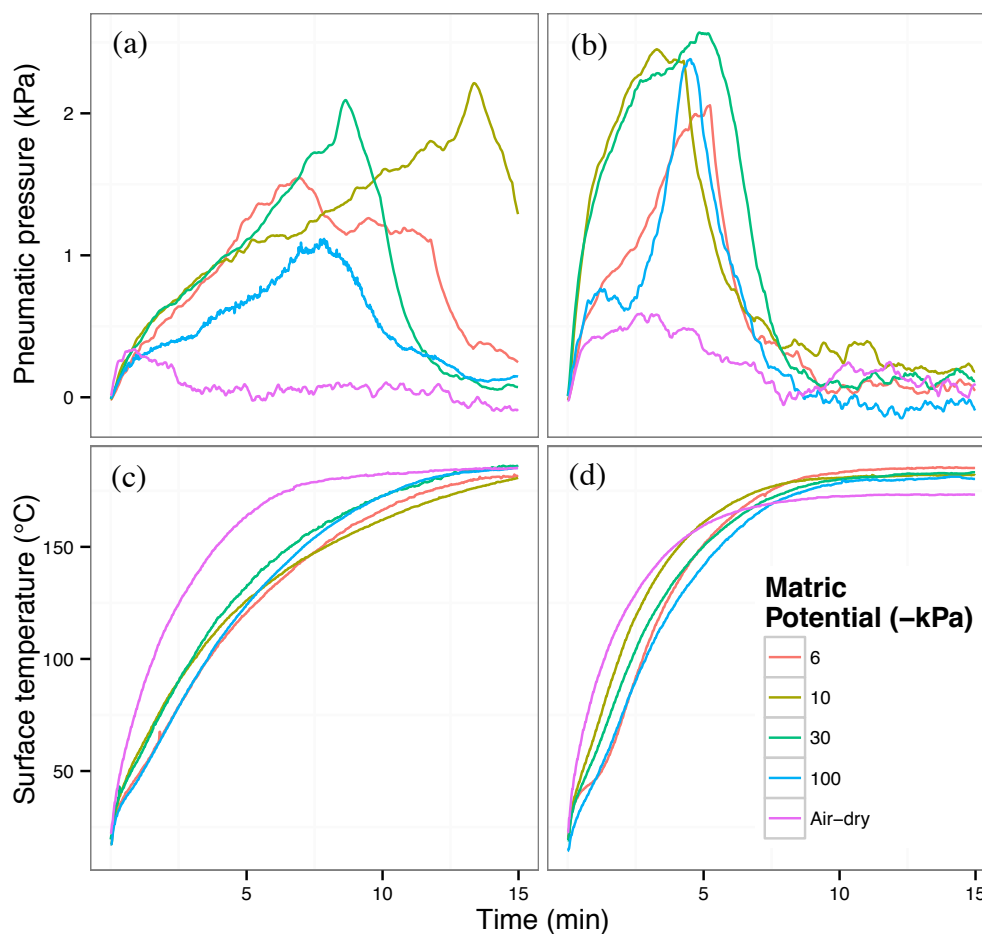


Figure 2-2 Example plots of the pneumatic gas pressure rise inside the (a) forest and (b) shrubland soil, and soil surface temperature of the (c) forest and (d) shrubland soil during heating experiment. Air-dried matric potentials for the forest and shrubland soil are -94,230 kPa and -123,603 kPa, respectively

The maximum pneumatic pressure observed inside the soil aggregates during the heating experiment and the soil aggregate tensile strength are shown in Figure 2-3. The plots for the forest and shrubland soil are plotted on the left and right, respectively. For

all the data points, the standard error of multiple replicates is indicated with error bars. For the forest soils, a total of 24 measurements was taken over the five matric potentials. For the shrubland soils, a total of 27 measurements was taken over the five matric potentials. During the heating experiment, we expected to see higher maximum pneumatic pressure with increasing initial soil aggregate moisture content. This is due to the higher initial soil moisture producing more water vapor that can become trapped within the aggregate to produce higher pneumatic pressure. We also expected the tensile strength of the soil aggregates to decrease with increasing initial soil aggregate moisture content.

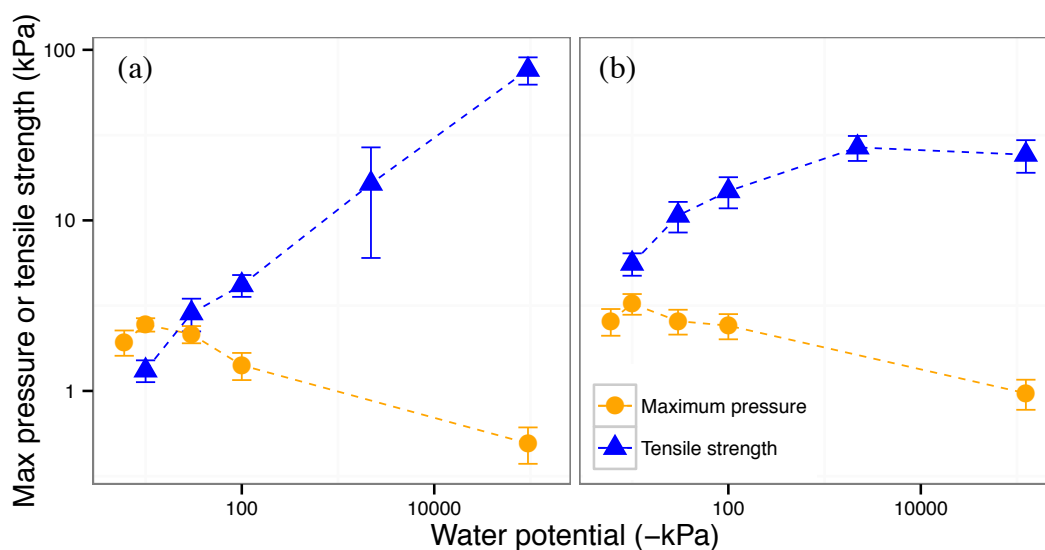


Figure 2-3 Maximum internal pressure and tensile strength of (a) forest and (b) shrubland soil over multiple matric potentials. Values are averaged of between 7 and 20 replicates for the maximum pneumatic stress measurements, and between 3 and 11 replicates for the tensile strength measurements, with error bars representing standard error in the y-axis

The range of predicted viscous strain from the pneumatic pressure rise on the soil aggregates during the heating experiment at multiple matric potentials during the heating experiment are given in Figure 2-4. The plots for the forest and shrubland soil are plotted on the left and right, respectively. The maximum predicted viscous strains in Figure 2-4 corresponds to the average maximum predicted viscous strain plus one standard deviation, and the minimum predicted viscous strains in Figure 2-4 corresponds to the average minimum predicted viscous minus one standard deviation.

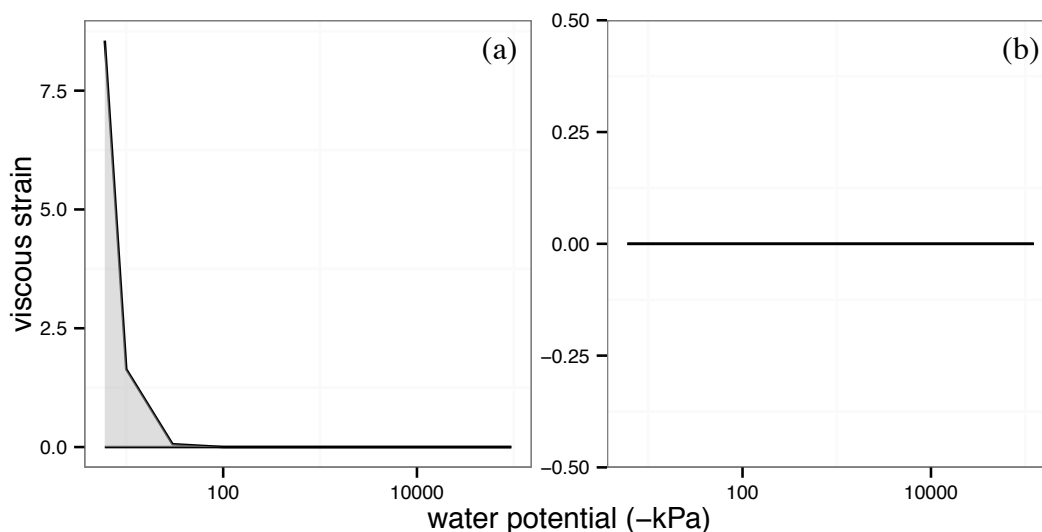


Figure 2-4 The range of predicted viscous strain experienced by (a) forest and (b) shrubland soil due to pneumatic gas pressure increase during the heating experiment. Note the y-axis scale is not the same for both of the plots

The range of predicted elastic strain from the pneumatic pressure rise on the soil aggregates during the heating experiment at multiple matric potentials during the heating experiment are given in Figure 2-5. The plots for the forest and shrubland soil are plotted

on the left and right, respectively. The maximum predicted elastic strains in Figure 2-5 corresponds to the average maximum predicted elastic strain plus one standard deviation, and the minimum predicted elastic strains in Figure 2-5 corresponds to the average minimum predicted elastic minus one standard deviation.

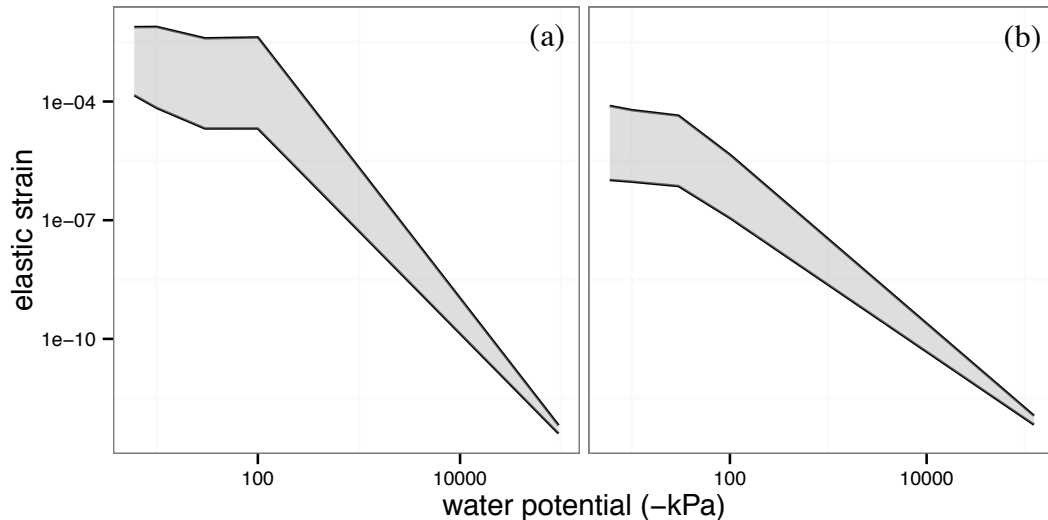


Figure 2-5 The range of predicted elastic strain experienced by (a) forest and (b) shrubland soil due to pneumatic gas pressure increase during the heating experiment.

2.4 Discussion

2.4.1 Micromechanical experiment and modeling of aggregate degradation

The tensile strength test in our study shows values that are comparable to others from literatures that use different methods. Most studies use a crushing method to determine the tensile strength of soil aggregates (Dexter and Kroesbergen, 1985). For example, Causarano (1993) developed a linear regression model for sandy loam soil aggregate tensile strength as a function of gravimetric water content after determining the

tensile strength using a crushing method . Using the equation, the tensile strength of soil aggregates with gravimetric water contents of 0.359 and 0.311 g water per g soil (the gravimetric water content of the Mariposa soil at -10 and -100 kPa matric potential, respectively) is calculated to be 2.85 kPa and 3.33 kPa, respectively. This is comparable to the same order of magnitude as the Mariposa soil aggregates at 1.32 kPa and 4.17 kPa, respectively. Munkholm et al (2002) used a similar method as Dexter and Kroesbergen (1985) and showed that large sandy loam soil aggregates at matric potential of -30 kPa had a tensile strength of around 7 kPa, comparable to the 2.85 kPa tensile strength of the Mariposa soil aggregates at -30 kPa matric potential. The results of our tensile strength test confirms that moist soil aggregates are inherently weaker than dry soil aggregates and can possibly break down when subjected to pneumatic gas pressure increase from rapidly vaporized soil moisture.

Soil moisture can induce loss of soil structural stability during low intensity burns in two ways (Albalasmeh et al., 2013). First, vaporization of soil moisture can potential induce rapid rise in pneumatic gas-pressure. Second, the soil tensile strength increases as soil dries. Therefore, initially moist soil aggregates are more likely to breakdown from the rapidly vaporized soil moisture while the strength of the moist soil aggregates are still low. Our results confirm that pneumatic gas pressure does increase significantly higher for initially moist soil aggregates than initially dry soil aggregates, and tensile strength of soil aggregates increase as soil dries, as shown in Figure 2-3. Albalasmeh et al. (2013) showed that rapid vaporization of soil moisture from soil aggregates initially at -300 kPa matric potential produced sufficient pneumatic gas pressure to disrupt the bonds between soil particles to decrease soil aggregate stability. While our study did not test soil

aggregates at such matric potential, the results suggest that sufficient pneumatic gas pressure was produced for the range of matric potentials in this study (-6 kPa to -100 kPa) to weaken the soil aggregates in this study.

The pressure increase within the soil aggregate can induce stress onto the soil aggregates as moist soil aggregate behave as a Bingham visco-plastic material (Ghezzehei and Or, 2000; Markgraf et al., 2006; Barre and Hallett, 2009). Although the stress is very miniscule, it can potentially cause strain to the soil aggregates that can cause microscopic breakdowns. This strain is evident in both Figure 2-4 and Figure 2-5. For the forest soils, the predicted viscous strain can be as high as 8.55 for the wettest moisture condition. However, the predicted viscous strain for the shrubland soil was zero. Yet, the predicted elastic strain caused by the stress for both of the soil increases exponentially with increasing moisture content. This further shows that the wetter the soils are initially before a burn, the more damage the vaporized water can weaken the soil aggregates. It is important to note that the modeling exercise is a semi-quantitative indication of the deformation of the soil aggregates, as the model parameters used for predicting viscous and elastic strain are based on fitting the model parameters to previous literature values in Ghezzehei and Or (2001). Nonetheless, the strain caused by the stress will most likely still be evident, but with varying degree depending on the rheological properties of the soil.

We acknowledge that there are other physical factors that may contribute to micromechanical breakdown of bonds between soil particles that were not addressed in this article. Some of these factors include desiccation of soil organic matter and other binding agents, thermal expansion of soil pore water, and differential thermal expansion

of mineral constituents. All of these can create localized tensile stresses at the particle-to-particle contact points, which can lead to failure of aggregate bonds. However, it may be a combination of all of these factors and the pore pressure rise within the aggregate that contribute to micromechanical breakdown of aggregates. We suggest that future studies test for the combination of some or all of the listed factors.

2.4.2 Implications of Prescribed Burns for Ecosystem Processes

Controlled burns are generally low in intensity and severity to minimize the negative effects on soils and ecosystem processes. This is typically done by conducting the burns in conditions when soil moisture levels are moderate to high (Carter and Foster, 2004; Certini, 2005; USDA, 2012). However, the experimental results suggest that it is best to conduct controlled burns in drier soil moisture conditions to minimize soil structural degradation from pneumatic steam pressure from rapidly vaporized soil moisture.

This underappreciated mechanism of soil aggregate degradation can have significant repercussions on ecosystem processes that may be overlooked. For example, the loss of soil structure through disaggregation and collapse of large pores can result in decrease in total porosity and increase in bulk density (Chief et al., 2012). Additionally, the sealing of macropores following burns can result in decrease in hydraulic conductivity and infiltration (Scott and Burgy, 1956). This post-burn soil sealing can further be aggravated by breakdown of already weakened soil aggregates due to raindrop impacts that results in soil surface compaction (Poesen and Savat, 1981; Hoogmoed and Stroosnijder, 1984). The weakening and breakdown of aggregates can also play a

significant role in soil organic matter decomposition, as soil organic matter decomposition is primarily controlled by physical accessibility of organic matter to decomposers (Gaillard et al., 1999; Schmidt et al., 2011).

Besides ecosystem processes, such mechanism of soil disaggregation can also have significant effects on human society. For example, the decreased infiltrability and post-fire sealing can result in higher soil erosion rate in the burned landscape. This increase in erosion can be of concern because of potential decrease in site productivity and adverse effects on downstream resources such as water quality and transported sediment (Benavides-Solorio and MacDonald, 2005). Soil aggregate degradation by this mechanism can also potentially occur in slash-and-burn agriculture, which is practiced by many rural and indigenous communities in developing countries (Kleinman et al., 1995). This loss in soil aggregation can decrease the soil from slash-and-burn agriculture's capability to retain soil moisture and nutrients (Horn and Smucker, 2005).

Improved understanding of how low intensity fires alter soil aggregation and the associated landscape and ecosystem processes is crucial in designing protocols of prescribed burns that minimize these effects. Furthermore, low severity burns have been shown to account approximately half of the combined wildfire and prescribed burn areas reported in the U.S. between 1984 and 2014 (Eidenshink et al., 2007; MTBS, 2017). Therefore, soil alterations caused by low intensity burns should not be treated as a negligible effect, and we recommend that more studies look into the effects of low intensity fires on soil alteration.

2.5 Conclusion

For both types of soil aggregates, pneumatic pressure increase due to trapped vaporized soil moisture was observed in the soil aggregates during the heating experiment. Moreover, minimal amount of pressure increase was observed for the air-dried soil aggregates, whereas maximum pressure observed increased with initial soil moisture content. This suggests that vaporized moisture trapped within soil aggregates is the main cause of the pressure increase. This pressure increase can induce stress onto soil aggregates. Although the stress is very miniscule, it can potentially cause strain to the soil aggregates that can then cause microscopic breakdowns. These breakdowns can have potential implications for ecosystem processes, such as decreases in hydraulic conductivity and infiltrability, as well as change in soil organic matter decomposition. These types of effects will most likely be prominent in areas where controlled burns are conducted, since these burns are generally conducted during the wettest soil conditions. The results in this study suggest that it may be advantageous to conduct controlled burns during drier soil conditions. But it is important to weigh in the implications of dry soil conditions and burn severity.

Chapter 3

Mechanism of exposing physically protected soil organic carbon to decomposition by breakdown of soil aggregates during low intensity burns

Abstract

Soil aggregate degradation by medium and high intensity fires is often attributed to loss of soil organic matter, whereas low intensity fires are often considered benign to soil aggregate degradation due to the relative stability of the organic binding agents at these low temperature burns. Because of this, there are limited studies specifically focusing on the effect of low intensity fires on soil aggregation. However, recent studies suggest that conducting low intensity burns in moist soil conditions may accelerate soil aggregate degradation due to rapid vaporization of soil pore water that can induce stress on the soil aggregates. Such degradation of soil aggregates may expose physically protected organic carbon to decomposition. Here we show that for a forest soil aggregate, rapidly burning moist soil aggregates causes soil aggregate degradation that increased cumulative carbon mineralization when compared to aggregates that were unburned, aggregates that were dried when burned, and moist soil aggregates that were slowly

burned. This was due to the exposure of previously physically protected organic carbon within the soil aggregates to oxidative conditions. Additionally, we show that for a shrubland soil aggregate with relatively low organic carbon content, low intensity burns increased cumulative carbon mineralization. We hypothesized that this was due to decomposition of cytoplasmic material from lysed microbes. Our results suggest that low intensity burns can accelerate decomposition of soil organic carbon protected in soil aggregates.

3.1 Introduction

Soil aggregation (or structure) is one of the most important soil qualities as it has significant control over many physical, chemical, and biological processes in both natural and anthropogenically-altered soils. Soil aggregates can serve to retain soil moisture and nutrients (Horn and Smucker, 2005), as well as house large inter-aggregate pore spaces that provide effective pathways for gas exchange for soil flora and fauna (Ghezzehei, 2012). However, intra-aggregate pores can be completely deprived of oxygen (Horn and Smucker, 2005), which can lead to the slow down of organic carbon decomposition (Balesdent et al., 2000). Micropores within aggregates can also serve to protect bacteria from predation by microfauna (Heynen et al., 1988), which can help to limit mineralization of carbon and nitrogen (Rutherford and Juma, 1992). For these reasons and many more, management practices often suggest protection of soil structure as it can help to enhance nutrient recycling, water availability, biodiversity, and sequestration of carbon (Bronick and Lal, 2005).

The ability of decomposers to decompose soil organic matter is primarily controlled by the physical accessibility of the organic substance. This can include the physical distances between the substrates and decomposers (Gaillard et al., 1999), short-distance transport processes of labile organic matter to decomposers (or vice versa) (Ekschmitt et al., 2008), and physical disconnection of water-saturated and unsaturated pore spaces (Schmidt et al., 2011). Moreover, decomposition is also controlled by the availability of resources such as oxygen (Ekschmitt et al., 2008), water and nutrients (Marschner and Kalbitz, 2003; Bachmann et al., 2008). This means that soil organic matter decomposition occurs where the substrate, decomposers, oxygen, water, and nutrients occupy the same space. Soil structure plays an important role in stabilization of soil organic matter by protecting the organic matter within soil aggregates and physically isolating the soil organic matter from soil decomposers (Hassink and Whitmore, 1997; Piccolo and Mbagwu, 1999; Balesdent et al., 2000).

The mechanisms of physical protection of soil organic matter within soil aggregates have been the subject of numerous recent investigations. Soil organic matter have been shown to be encrusted by minerals when viewed under transmission electron microscopy (Chenu and Plante, 2006). It has been shown that in soils that have been subjected to decades of maize cropping, organic carbon that is occluded within aggregates had significantly longer turnover time than bulk soil organic carbon, and may contain up to 80% of the soil organic carbon (Flessa et al., 2008). As reviewed by Balesdent et al. (2000), there are various mechanisms of physical protection of soil organic matter within aggregates. These may include adsorption of soil organic matter to solid surfaces, pockets of water-saturated pores within soil structural units that slow

decomposition by limiting oxygen, and complex pore geometry and tortuosity of diffusion pathways that limit diffusion of soil organic substrate to soil decomposers.

One particular, but understudied, way that soil aggregates can physically break up is from stress applied onto soil aggregates by rapidly vaporized soil pore water from initially wet soil aggregates during low intensity burns, as studied by Albalasmeh et al. (2013) and in chapter two of this thesis. Their studies were partly motivated by observations made on the soil structure of a shrubland in the eastern Great Basin in Nevada a year after a controlled, low intensity burn (Chief et al., 2012; Kavouras et al., 2012). The soil structure degraded from having a blocky structure to structure over a course of nine to 13 months after the burn. This is of particular importance as Albalasmeh et al. (2013) was the first to suggest this mechanism of soil aggregate degradation during low intensity burns (Urbanek, 2013), and only a limited number of studies have focused on the effects of low intensity fires on soils as they are presumed to have minor effects on landscape and ecosystem processes (DeBano et al., 1977; Mataix-Solera et al., 2011), and soil carbon and nitrogen content (Moghaddas and Stephens, 2007).

The foregoing observations suggest that soil structural degradation by stress applied onto soil aggregates by rapidly vaporized soil pore water during low intensity burns may expose previously physically protected soil organic matter to decomposition. Therefore, we hypothesize that rapidly burned moist soil aggregates may experience higher amount of carbon mineralization. We tested this hypothesis by (1) comparing the amount of mineralized carbon in soil aggregates subjected to identical final temperature using rapid and slow heating rates, and (2) compare the chemical characteristics of the dissolved organic carbon across the heating treatments, as dissolved organic matter is the

most bioavailable fraction of soil organic matter since majority of microbial uptake mechanisms require water (Marschner and Kalbitz, 2003). The present work will attempt to address that the presumed minor effects that low intensity burns have on landscape and ecosystem processes may have severely limited the knowledge of such burns on organic matter decomposition.

3.2 Methods

3.2.1 Soil Collection

Soils were collected from two distinct ecosystems that experience low severity fires in the western United States. The first soil was a sandy loam collected from an undisturbed pine forest in Mariposa County, United States. The second soil was a loam collected from an unburned shrubland (adjacent to the burn boundary of the Carpenter 1 Fire) in Clark County, United States. In the subsequent sections of this paper, these soils will be referred to as forest and shrubland soils, respectively.

Soil samples were collected from 0-10 cm depth, air dried, and then separated into three aggregate size fractions (0.25-1 mm, 1-2 mm, and 2-4 mm) by dry sieving. The separated fractions were then homogenized by gentle mixing with hands. Characteristics of the soils are provided in Table 3 – 1.

Table 3-1 Characterization of studied soils (mean \pm standard error, where n = 3 to 5. Clay content is expressed in mean \pm standard deviation, where n = 4 for forest soil and n = 3 for shrubland soil)
*Value previously reported by Albalasmeh et al (2013)

Soil	Aggregate size (mm)	Field capacity water content (g/g)	Organic Carbon (%)	Clay (%)
Forest	0.25 to 1	0.328 \pm 0.001	5.73 \pm 0.07	11.55 \pm 4.90*
	1 to 2	0.252 \pm 0.003	4.67 \pm 0.10	
	2 to 4	0.286 \pm 0.012	3.58 \pm 0.10	
Shrubland	0.25 to 1	0.165 \pm 0.002	1.25 \pm 0.02	21.05 \pm 0.86
	1 to 2	0.145 \pm 0.001	0.70 \pm 0.01	
	2 to 4	0.120 \pm 0.002	0.53 \pm 0.01	

3.2.2 Gravimetric Water Content of Soil Aggregates at Field Capacity

A set of triplicate 5 g of soil aggregate of each soil type and aggregate size was wetted by placing them on porous plates inside a pressure plate apparatus. The aggregates were wetted by lightly spraying a fine mist of water and subsequently being gradually wetted by capillary action from a thin film of water on top of the porous plates. After the aggregates were equilibrated to a water potential of -30 kPa (field capacity) for 24 hours, they were carefully transferred to aluminum weighing dishes and their gravimetric water content was determined by drying them in an oven at 105°C for 24 hours. The gravimetric water content of the soil aggregates is summarized in Table 3 – 1.

3.2.3 Dissolved organic carbon leaching experiment

3.2.3.1 Laboratory Heating Treatments

The goal of the dissolved organic carbon leaching experiment was to compare amount and characteristics of dissolved organic carbon in soil aggregates undergoing various low intensity heating treatments. To achieve this goal, soil aggregates wetted to field capacity were heated to 175°C at slow and rapid heating rates (SB and RB) inside

a muffle furnace with a heating-rate control. These samples were compared to unburned (UB) aggregates and air-dried aggregates burned (DRB) with the same heating treatment as the RB samples.

Prior to the heating treatments, 10 g of soil aggregates from the 2-4 mm size fraction per sample were added to stainless steel cups with plastic lids. Water was slowly added onto the SB and RB treatment of soil aggregates by lightly spraying with a fine mist of water to get the water content of the soil aggregates to field capacity. The cups were then capped and the samples were allowed to equilibrate for 16 h.

The SB treatment was carried out by placing the samples inside a muffle furnace at room temperature ($\sim 25^{\circ}\text{C}$) and subsequently raising the temperature at $\sim 3^{\circ}\text{C}/\text{min}$ until the furnace reached 175°C . The samples were then kept at this temperature for 30 minutes, which is equivalent to the time it takes for small dry logs to burn (Stoof et al., 2010). The RB and DRB treatment involved placing the aggregates inside the muffle furnace preheated to 175°C for 30 min. After the heating treatments, the soil aggregates were cooled in a dark cabinet at 21°C for 24 h. For each soil type, three to five replicate samples were subjected to their heating treatments.

3.2.3.2 Soil Leachate Collection and Analysis

Soil aggregates were transferred onto pre-saturated porous plates in a Tempe Cell set-up. Soil aggregates were then wetted by lightly spraying with a fine mist. 40 mL of deionized water was then slowly added into the Tempe Cell and the aggregates were allowed to soak for 15 min. Afterwards, 10 kPa of pressure was applied for 10 min to extract the soil leachate from the Tempe Cell. The leachate was then further filtered

through a 0.45 μm filter paper before being stored in the dark at 4°C for a maximum of 14 days. The dissolved organic carbon (DOC) concentration in the leachate was measured using a Shimadzu TOC-Vcsh analyzer.

Chemical composition of the soil leachate was analyzed using a Thermo Scientific Evolution 3000 Ultraviolet-Visible (UV-VIS) spectrophotometer. Absorbance was measured between 200 and 560 nm, using ultrapure water as blank. Measurements were performed using a quartz cell with 1.25 cm path length. The specific UV absorbance at 254 nm (SUVA_{254}) was used to determine whether there were changes in aromaticity of the DOC in the burned samples. SUVA_{254} was calculated by normalizing the specific absorbance coefficient at 254 nm by the DOC concentration. The ratio of absorption at 250 nm to 365 nm ($A_{250}:A_{365}$) was used to deduce the average molecular size of the organic carbon in the soil leachate as high molecular weight molecules absorb light at longer wavelengths than at shorter wavelengths (Santos et al., 2016).

3.2.4 CO₂ Respiration Rate

3.2.4.1 Laboratory Heating Treatments

The goal of the heating treatment was to test whether degradation of aggregate stability from elevated steam pressure generated by rapid vaporization can lead to higher rates of soil organic carbon mineralization. Prior to the heating treatment, 5 g of soil aggregates in the 0.25-1 mm and the 1-2 mm size fraction per sample were added into 50 mL glass vials with caps equipped with rubber septa. Water was slowly added onto the SB and RB treatment of soil aggregates using a micropipette to get the water content of the soil aggregates to field capacity. The caps were then sealed and the

samples were allowed to equilibrate for 16 h.

The SB treatment was carried out by placing the samples inside a muffle furnace at room temperature ($\sim 25^{\circ}\text{C}$) and subsequently raising the temperature at $\sim 3^{\circ}\text{C}/\text{min}$ until the furnace reached 175°C . The samples were then kept at this temperature for 30 minutes, which is equivalent to the time it takes for small dry logs to burn (Stoof et al., 2010). The RB and DRB treatment involved placing the aggregates inside the muffle furnace preheated to 175°C for 30 min. After the heating treatments, the soil aggregates were cooled in a dark cabinet at 21°C for 24 h. For each combination of soil type and aggregate size, four or five replicate samples were subjected to their heating treatments.

3.2.4.2 *CO₂ Measurements*

The samples were then wetted to field capacity with a micropipette and then capped and allowed to equilibrate for 24 hours. Afterwards, the caps were removed and the vials were covered with Parafilm and incubated at 21°C in the dark for over two months. The vials were weighed every 3-7 days and water was added to maintain the initial moisture content. Gas samples were pulled from the forest sample vials on days 1, 2, 3, 5, 7, 10, 13, 17, 21, 26, 31, 37, 43, 50, 57, and 65 by capping the vial for 3 hours and extracting 15 mL of gas through septa on the vial caps. Gas samples were pulled from the shrubland samples in a similar fashion on days 1, 2, 3, 5, 7, 10, and 13. The samples were then analyzed on a gas chromatograph (Shimadzu GC-2014) fitted with a thermal conductivity detector to determine the concentration of carbon dioxide.

3.2.4.3 *Soil Organic Carbon Mineralization Rate*

The change in soil organic carbon stock due to mineralization can be described

using a “one-pool” model (Jenny, 1980)

$$\frac{dC}{dt} = -kC \text{ (Eq. 3.1)}$$

where C (C-mass/ soil-mass) is the quantity of mineralizable C and k (1/time) is the rate constant of mineralization. Assuming steady state conditions and that the soil remained under constant environmental conditions, the equation can be solved to provide an exponential decay of soil C content

$$C = C_0 e^{-kt} \text{ (Eq. 3.2)}$$

where C_0 is the biologically available C pool, and C is the stock of potentially mineralizable C at time t .

Thus, the total C mineralized at time t can be given as

$$C_t = C_0(1 - e^{-kt}) \text{ (Eq. 3.3)}$$

3.2.5 Statistical analysis

In order to determine the initial mineralizable C pool and the rate constant of mineralization, the cumulative C mineralized data was fitted to Eq. 3.3 with the exception of the forest SB and RB treatments. These samples were fitted to Eq. 3.7 as described in the subsequent sections.

Comparisons of burn treatments for DOC concentration, $SUVA_{254}$, and A250:A365 in the soil leachate, and initial mineralizable C pool and rate constant of mineralization of for the CO_2 measurements were performed using one-way ANOVA, and pairwise comparison of burn treatments was performed using Tukey’s test at $p < 0.05$ significance level when applicable. All analyses were conducted using R statistical software (r-project.org).

3.3 Results

3.3.1 Dissolved Organic Carbon concentration of leachate

The average DOC concentration of the leachate in the unburned (UB) forest soil was $34.4 \pm 0.4 \text{ mg L}^{-1}$ (Figure 3 – 1). Heating dried forest soil (DRB) significantly increased the DOC concentration when compared to the unburned treatment ($P < 0.05$, $83.3 \pm 1.3 \text{ mg L}^{-1}$). The rapidly heated (RB) and slowly heated (SB) had DOC concentration of $72.5 \pm 4.2 \text{ mg L}^{-1}$ and $91.4 \pm 4.2 \text{ mg L}^{-1}$, respectively. The RB and SB forest treatments had DOC concentrations that were significantly higher than UB treatment ($P < 0.05$) and significantly differed from each other ($P < 0.05$). Neither, however, was significantly different than the DRB treatment ($P > 0.05$).

The average DOC concentration of the leachate in the UB shrubland soil was $3.1 \pm 1.1 \text{ mg L}^{-1}$. The DRB, RB, and SB treatments had DOC concentrations of 20.0 ± 3.2 , 20.8 ± 1.4 , and $28.4 \pm 2.3 \text{ mg L}^{-1}$, respectively. All three treatments had DOC concentrations significantly higher than the UB treatment ($P < 0.05$). None of the DRB, RB, and SB treatments had DOC concentrations that significantly differed from each other ($P > 0.05$).

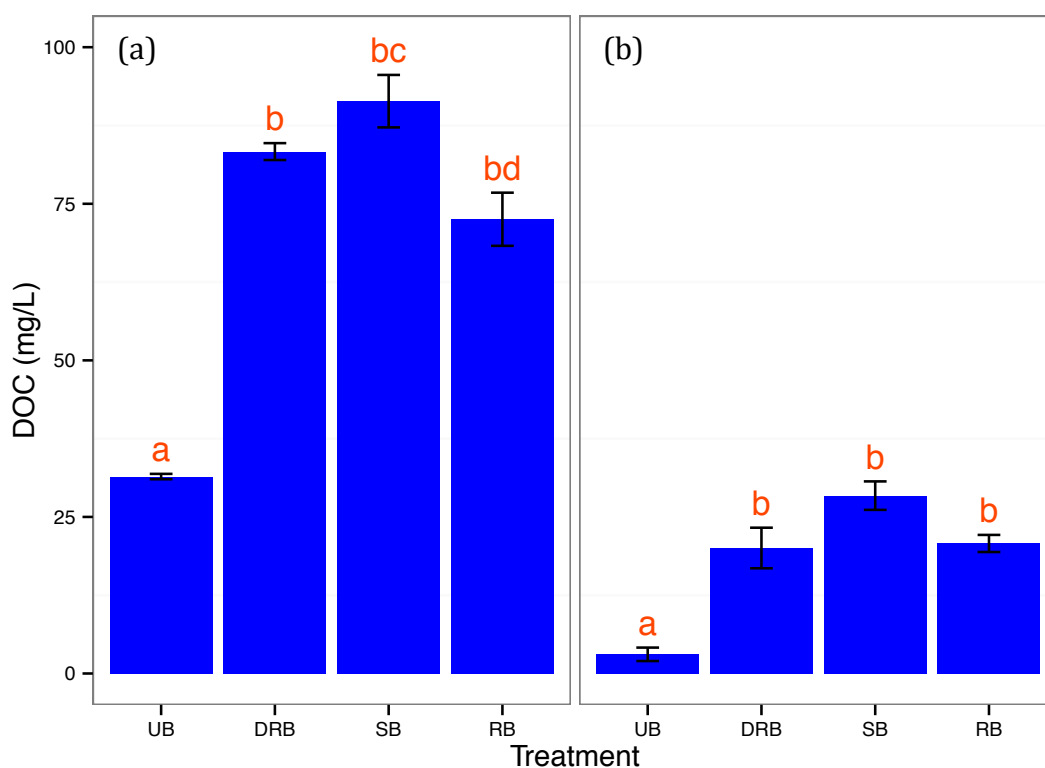


Figure 3-1 Dissolved organic carbon (mg L^{-1}) in the soil leachate from unburned (UB), rapidly burned dried (DRB), slowly burned (SB) and rapidly burned (RB) soil aggregates from (a) forest soil and (b) shrubland soil. Different letters represent significantly different means as determined from Tukey's HSD Test ($P < 0.05$)

3.3.2 Specific UV Absorbance of leachate

SUVA_{254} of UB treatment of forest soil was $1.26 \pm 0.03 \text{ L mgC}^{-1} \text{ m}^{-1}$ (Figure 3-2).

The DRB treatment of forest soil was not significantly different than the UB treatment ($P > 0.05$, $\text{SUVA}_{254} = 1.02 \pm 0.12 \text{ L mgC}^{-1} \text{ m}^{-1}$). The RB and SB treatment had SUVA_{254} of 0.92 ± 0.03 and $0.88 \pm 0.03 \text{ L mgC}^{-1} \text{ m}^{-1}$, respectively. The SUVA_{254} values for RB and SB treatment were significantly lower than the UB treatment ($P < 0.05$), but neither significantly differed from the DRB treatment ($P > 0.05$).

SUVA₂₅₄ of UB treatment of shrubland soil was $1.51 \pm 0.11 \text{ L mgC}^{-1} \text{ m}^{-1}$. The DRB, RB, and SB treatments had DOC concentrations of 0.82 ± 0.00 , 0.56 ± 0.07 , and $0.59 \pm 0.05 \text{ L mgC}^{-1} \text{ m}^{-1}$, respectively. All three treatments had SUVA₂₅₄ significantly lower than the UB treatment ($P < 0.05$). None of the three treatments had SUVA₂₅₄ that significantly differed from each other ($P > 0.05$).

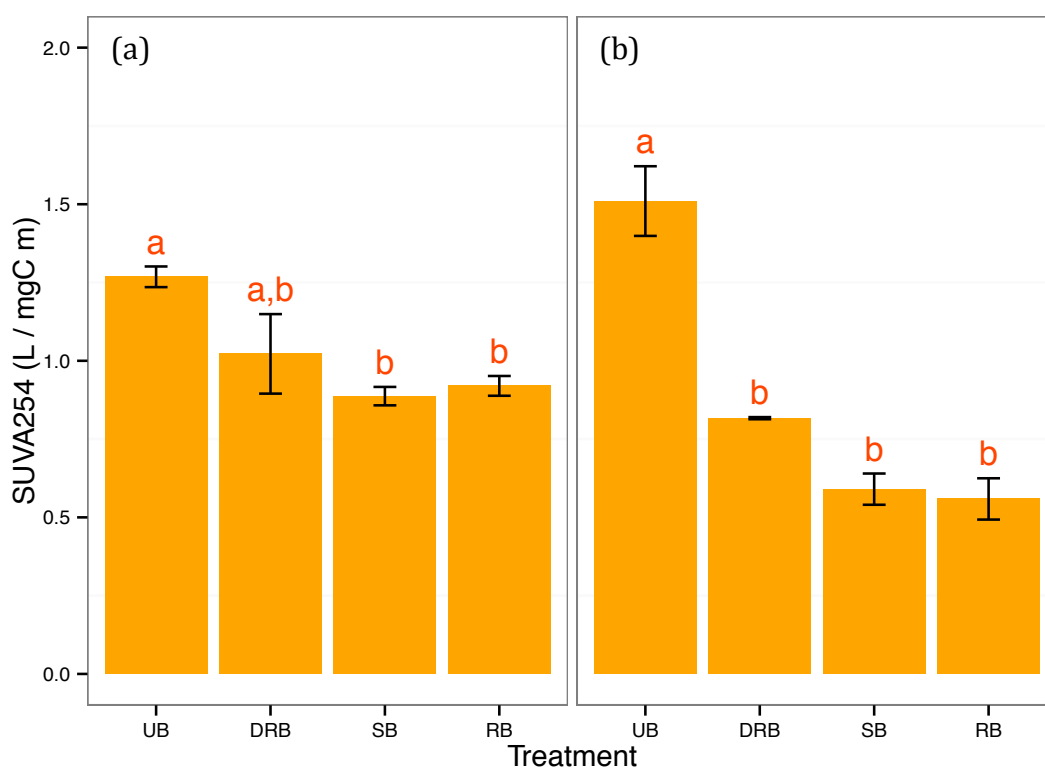


Figure 3-2 SUVA₂₅₄ in the soil leachate from unburned (UB), rapidly burned dried (DRB), slowly burned (SB) and rapidly burned (RB) soil aggregates from (a) forest soil and (b) shrubland soil. Different letters represent significantly different means as determined from Tukey's HSD Test ($P < 0.05$)

3.3.3 Average molecular size of dissolved organic carbon in leachate

The heating treatments did not appear to have a significant effect on the average molecular size of organic carbon in the forest soil leachate (Figure 3 – 3). A decrease in $A_{250}:A_{365}$ ratio indicates an increase in average molecular sizes. This appears to be the trend for RB and SB treatment in the shrubland soil with $A_{250}:A_{365}$ values of 5.9 ± 1.2 , and 6.2 ± 1.8 , respectively, and the UB treatment with an $A_{250}:A_{365}$ value of 15.9 ± 6.0 . However, none of the burn treatments had an average molecular size of DOC that significantly differed from each other ($P > 0.05$).

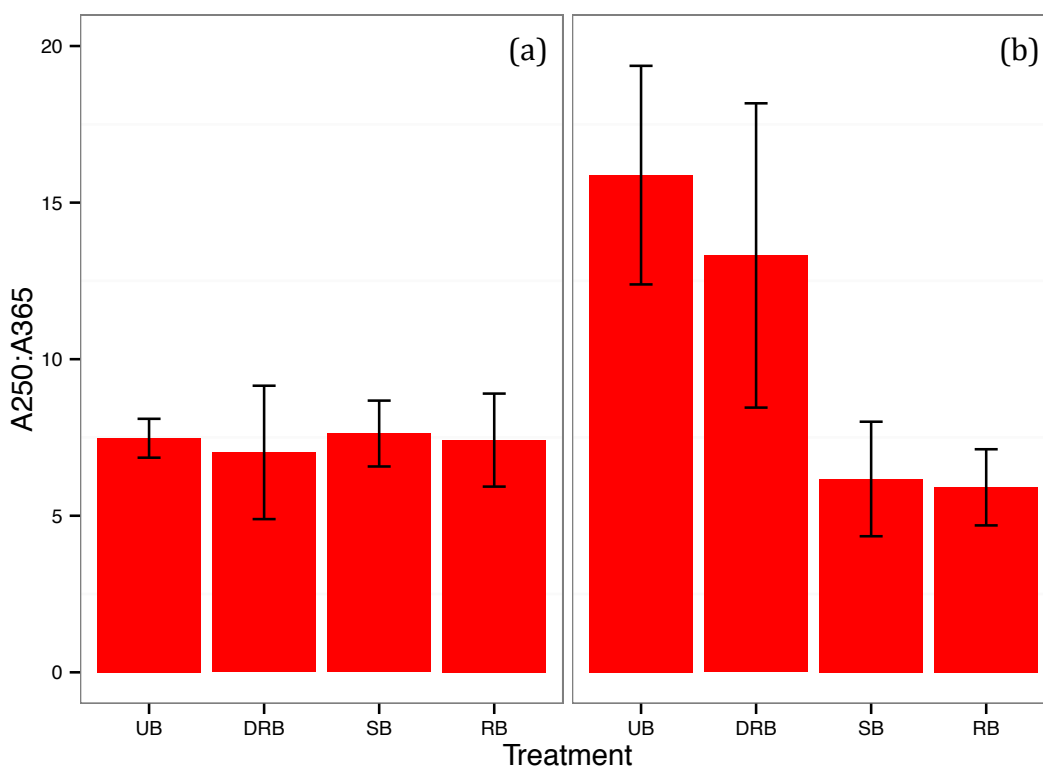


Figure 3-3 $A_{250}:A_{365}$ in the soil leachate from unburned (UB), rapidly burned dried (DRB), slowly burned (SB), and rapidly burned (RB) soil aggregates from (a) forest soil and (b) shrubland soil. No significant differences were found between burn treatments.

3.3.4 CO₂ measurements

For the SB and RB treatments of forest soil, there appeared to be a second pool of carbon that appeared later during the duration of the experiment. For this reason, the total C mineralized at time t can be given as the following:

$$C_{t1} = C_1(1 - e^{-kt}) \text{ (Eq. 3.4)}$$

$$C_{t2} = C_2(1 - e^{-k(t-t_2)}), \text{ for } t > t_2 \text{ (Eq. 3.5)}$$

where C_{11} is the amount of mineralizable C in the first pool of C and C_{12} is the amount of mineralizable C in the second pool carbon that appears at time t_2 . The total C mineralized at time t for these samples is

$$C_t = C_{t1} + C_{t2} \text{ (Eq. 3.6)}$$

and the initial mineralizable C pool C_0 is

$$C_0 = C_1 + C_2 \text{ (Eq. 3.7)}$$

Figure 3-4 and Figure 3-5 show the cumulative CO₂-C loss over the course of the CO₂ measurements for the individual forest and shrubland soil samples, respectively. Each individual samples were shown in order to highlight the high variability in respiration within aggregate sizes and heating treatments Figure 3-4.1d, Figure 3-5.1a, and Figure 3-5.1d. Analysis of the cumulative CO₂-C loss and rate constant of mineralization is shown in the succeeding paragraphs.

Figure 3-4 also serves to outline the variability in t_2 for the SB and RB treatment of the forest soil. The SB treatment of the forest soil had average t_2 values of 4.7 ± 0.7 and 4.2 ± 1.0 days for soil aggregates of size 0.25-1 mm, and 1-2 mm, respectively. The

RB treatment of the forest soil had average t_2 values of 21.1 ± 2.4 and 19.9 ± 1.8 days for soil aggregates of size 0.25-1 mm, and 1-2 mm, respectively.

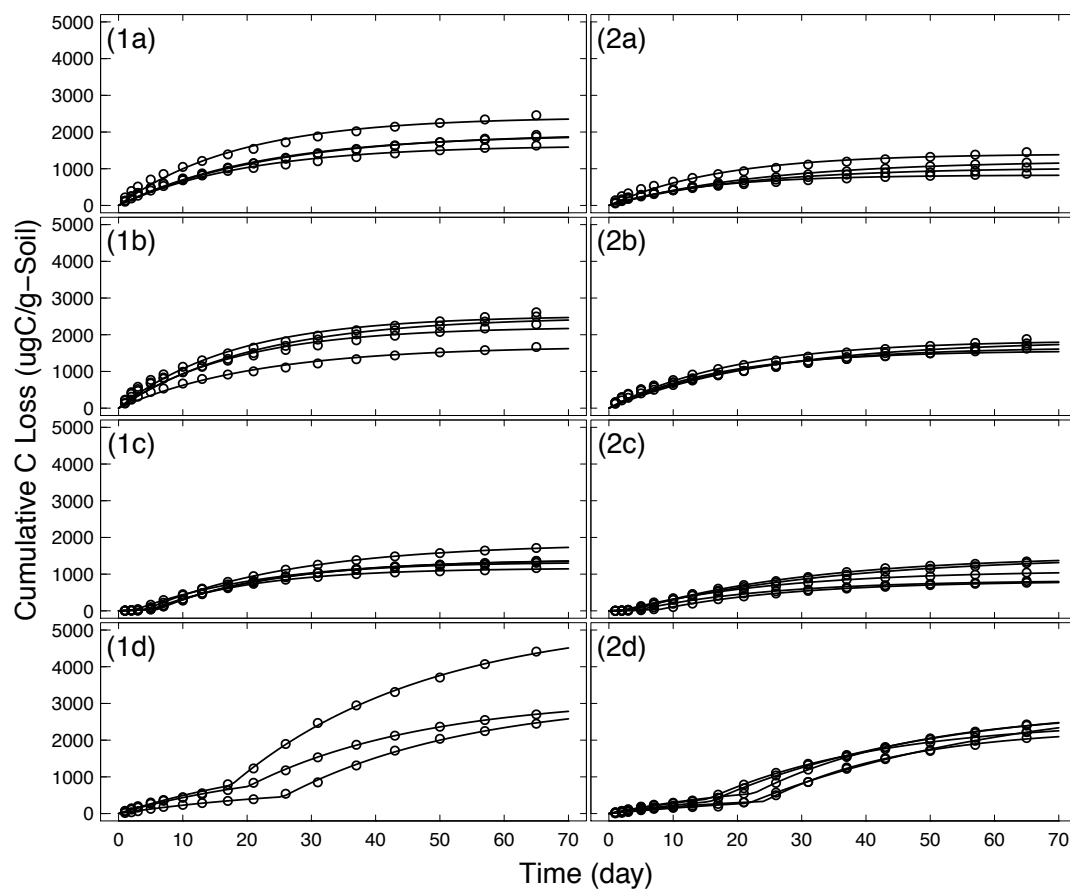


Figure 3-4 Cumulative $\text{CO}_2\text{-C}$ loss in $\mu\text{gC g soil}^{-1}$ for forest soil with aggregate sizes (1) 0.25-1 mm and (2) 1-2 mm. Rows (a-d) indicate UB, DRB, SB, and RB treatments, respectively.

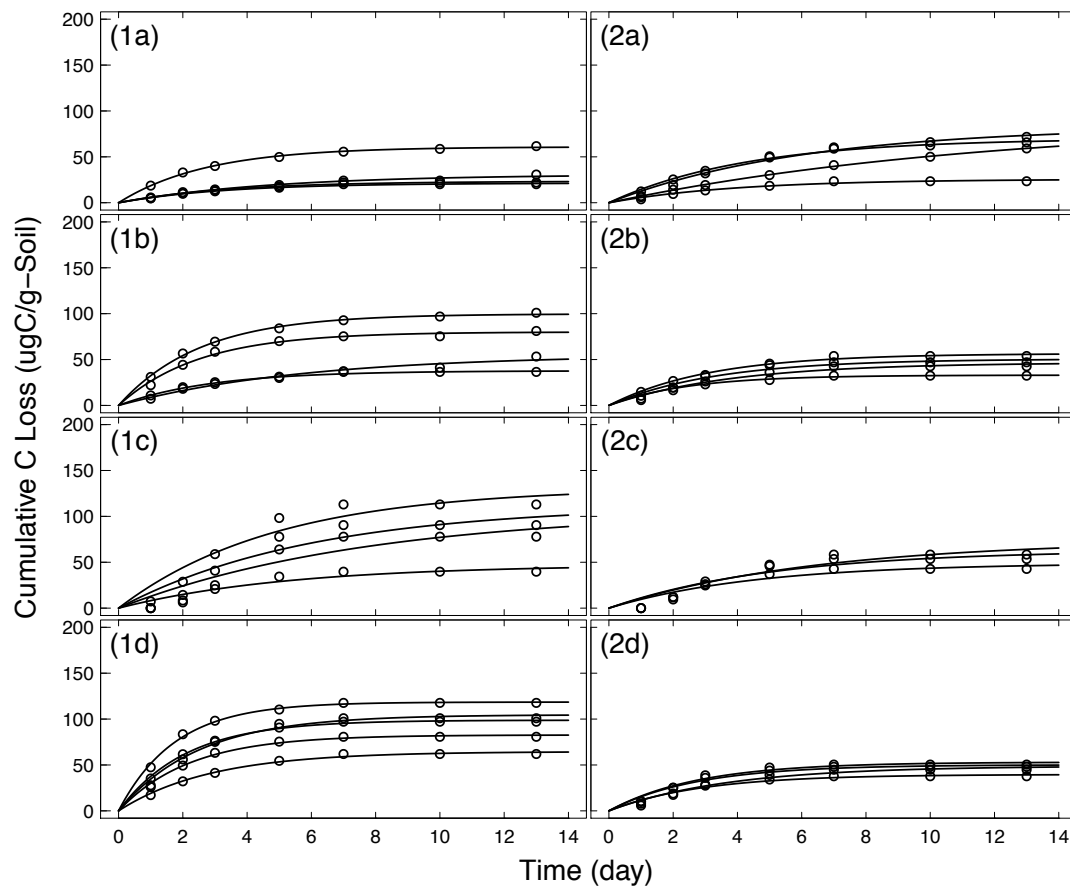


Figure 3-5 Cumulative $\text{CO}_2\text{-C}$ loss in $\mu\text{gC g soil}^{-1}$ for shrubland soil with aggregate sizes (1) 0.25-1 mm and (2) 1-2 mm. Rows (a-d) indicate UB, DRB, SB, and RB treatments, respectively.

C_0 of the UB treatment of forest soil with aggregate size from 0.25-1 mm was $1988.1 \pm 158.5 \mu\text{gC g soil}^{-1}$ (Figure 3-6). The DRB and SB treatment of forest soil with aggregate size 0.25-1 mm had C_0 of 2229.2 ± 192.7 and $1432.7 \pm 112.0 \mu\text{gC g soil}^{-1}$, respectively. Neither of these samples significantly differed from the UB treatment. The RB treatment has $C_0 = 3884.6 \pm 716.7 \mu\text{gC g soil}^{-1}$, which significantly differed from the other three treatments ($P < 0.05$). Similar summary was made for forest soil with aggregate size from 1-2mm in size ($P < 0.05$). The ratio of the biologically available pool

of carbon to the total carbon pool ($C_0:C_a$) follows the same trend (Figure 3-7) as C_0 to the treatments.

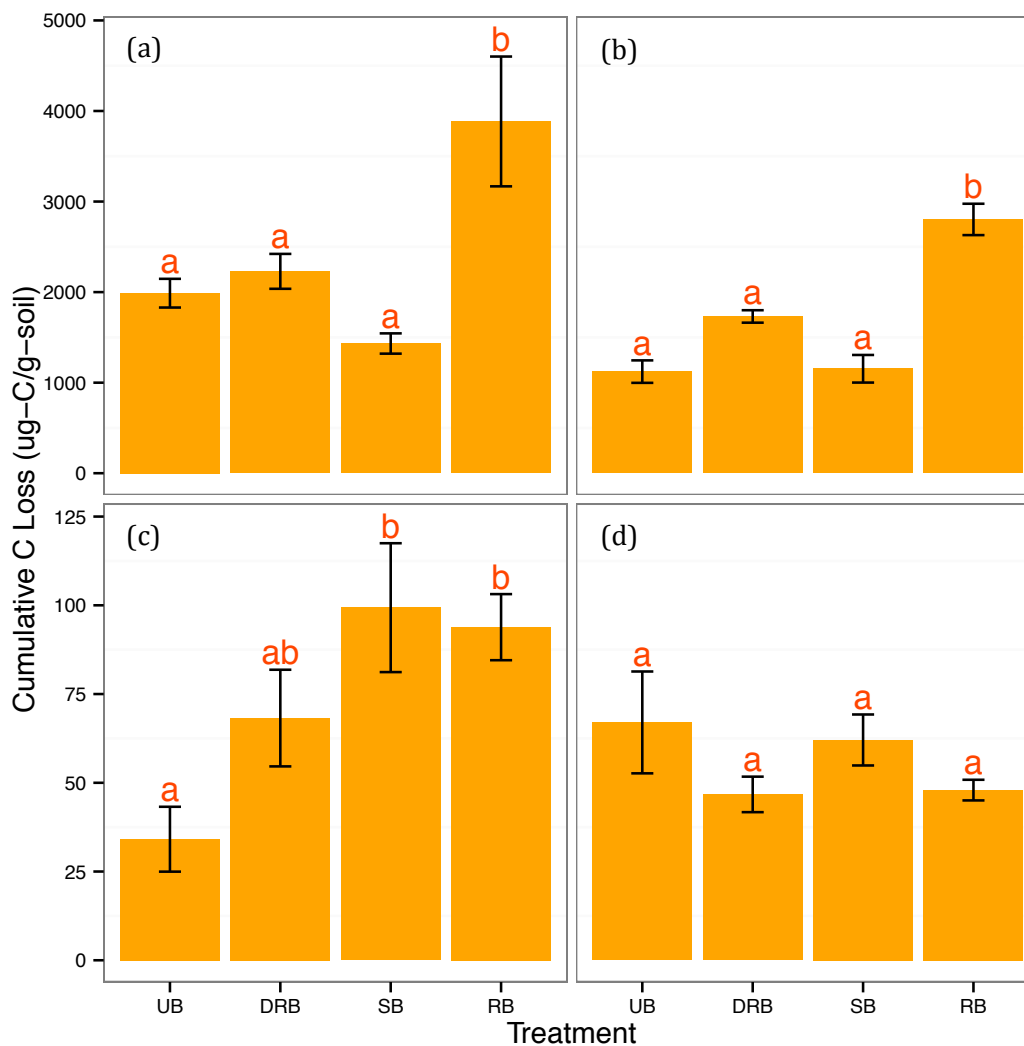


Figure 3-6 C_0 of unburned (UB), rapidly burned dried (DRB), rapidly burned (RB) and slowly burned (SB) soil aggregates from forest soil with aggregate sizes (a) 0.25 to 1 mm and (b) 1 to 2 mm, and shrubland soil with aggregate sizes (c) 0.25 to 1 mm and (d) 1 to 2 mm. Different letters represent significantly different means as determined from Tukey's HSD Test ($P < 0.05$)

C_0 of the UB treatment of shrubland soil with aggregate size from 0.25-1 mm was $34.1 \pm 9.1 \mu\text{gC g soil}^{-1}$. The DRB sample had C_0 that did not significantly differ from the UB treatment ($68.3 \pm 13.6 \mu\text{gC g soil}^{-1}$, $P > 0.05$). The SB and RB samples had C_0 values of 99.3 ± 18.2 and $93.8 \pm 9.3 \mu\text{gC g soil}^{-1}$, respectively. The SB and RB treatments had C_0 that were significantly higher than the UB treatment ($P < 0.05$). Neither of the samples significantly differed from the DRB treatment. For the shrubland soil with aggregate size from 1-2 mm, none of the treatments significantly differed each other ($P > 0.05$, $67.0 \pm 14.3 \mu\text{gC g soil}^{-1}$, $46.7 \pm 5.0 \mu\text{gC g soil}^{-1}$, $62.1 \pm 7.2 \mu\text{gC g soil}^{-1}$, $47.9 \pm 2.9 \mu\text{gC g soil}^{-1}$ for the UB, DRB, SB, and RB treatment, respectively). The ratio of the biologically available pool of carbon to the total carbon pool ($C_0:C_a$) follows the same trend (Figure 3-7) as C_0 to the treatments.

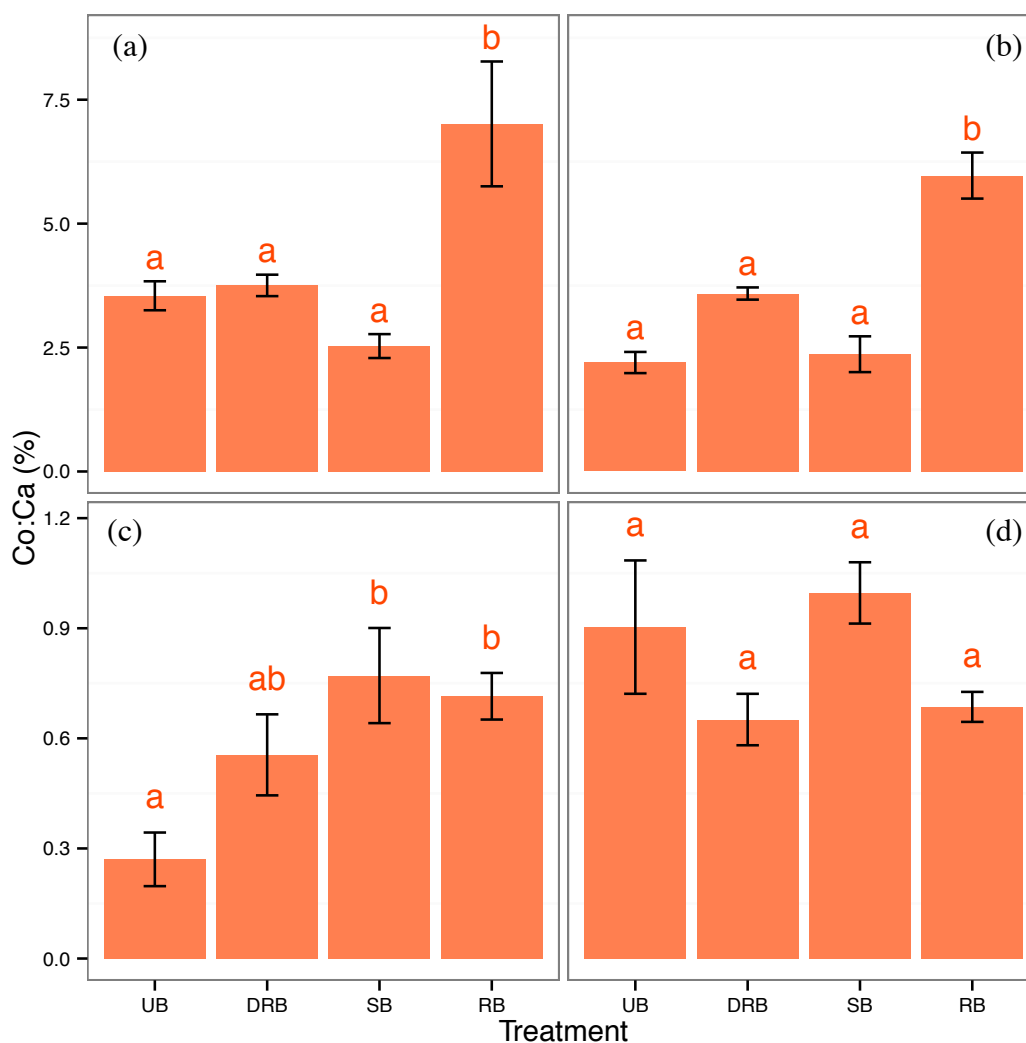


Figure 3-7 $C_0:C_a$ (the ratio of the biologically available carbon pool to the total carbon pool (C_a)) of unburned (UB), rapidly burned dried (DRB), rapidly burned (RB) and slowly burned (SB) soil aggregates from forest soil with aggregate sizes (a) 0.25 to 1 mm and (b) 1 to 2 mm, and shrubland soil with aggregate sizes (c) 0.25 to 1 mm and (d) 1 to 2 mm. Different letters represent significantly different means as determined from Tukey's HSD Test ($P < 0.05$)

k of the UB treatment of forest soil with aggregate size from 0.25-1 mm was $0.048 \pm 0.003 \text{ day}^{-1}$ (Figure 3-8). The DRB, SB, and RB treatments had k values of $0.051 \pm 0.002 \text{ day}^{-1}$, $0.052 \pm 0.004 \text{ day}^{-1}$, and $0.035 \pm 0.001 \text{ day}^{-1}$, respectively. None of the three treatments significantly differed from the UB treatment ($P > 0.05$), but the RB

treatment significantly differed from the DRB and SB treatment ($P < 0.05$). The UB treatment of forest soil with aggregate size from 1-2 mm was $0.053 \pm 0.006 \text{ day}^{-1}$. The DRB and SB treatment did not significantly differ from the UB treatment ($P > 0.05$, $0.049 \pm 0.007 \text{ day}^{-1}$ and $0.040 \pm 0.003 \text{ day}^{-1}$, respectively). The RB treatment significantly differed from the UB treatment ($P < 0.05$, $0.035 \pm 0.004 \text{ day}^{-1}$), but did not significantly differ from the DRB and SB treatment ($P > 0.05$).

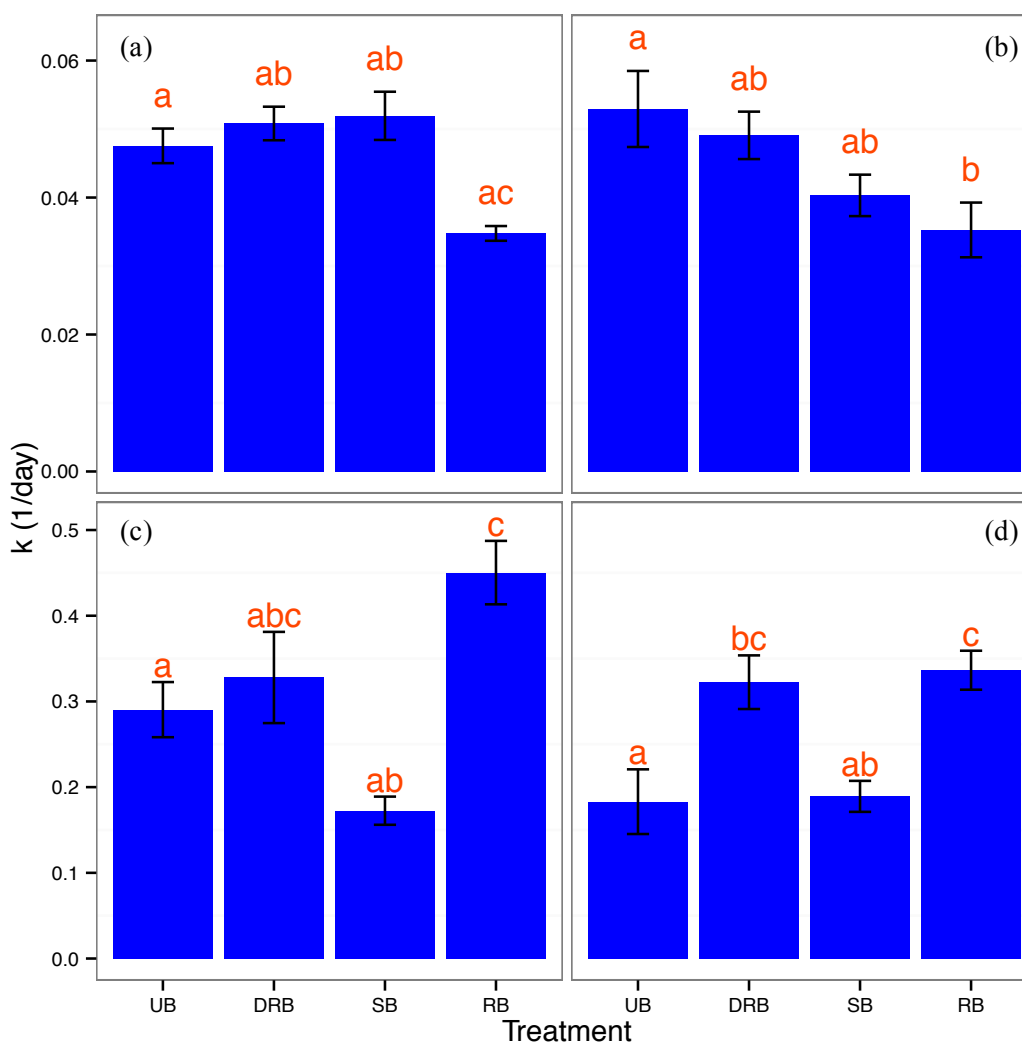


Figure 3-8 k of unburned (UB), rapidly burned dried (DRB), rapidly burned (RB) and slowly burned (SB) soil aggregates from forest soil with aggregate sizes (a) 0.25 to 1 mm and (b) 1 to 2 mm, and shrubland soil with aggregate sizes (c) 0.25 to 1 mm and (d) 1 to 2 mm. Different letters represent significantly different means as determined from Tukey's HSD Test ($P < 0.05$)

k of the UB treatment of shrubland soil with aggregate size from 0.25-1 mm was $0.290 \pm 0.032 \text{ day}^{-1}$. The DRB and SB treatments had k values of $0.328 \pm 0.053 \text{ day}^{-1}$, and $0.173 \pm 0.016 \text{ day}^{-1}$, respectively. Both of these treatments did not significantly differ from the UB treatment. The RB treatment had $k = 0.450 \pm 0.037 \text{ day}^{-1}$, which was

significantly higher than the UB treatment ($P < 0.05$), but was not significantly higher than the DRB treatment ($P > 0.05$). A similar trend is observed for shrubland soil with aggregate size from 1-2 mm. However, DRB treatment differed significantly from the UB treatment ($P < 0.05$).

3.4 Discussion

3.4.1 Dissolved organic carbon analysis in soil leachate

The increase in the amount of DOC across all of the burn treatments when compared to the UB control is consistent with previous soil heating studies. For example, Santos et al (2016) and Choromanska and DeLuca (2002) saw an increase in DOC when burning soils at around 150°C and 250°C. Increase in DOC concentration have been seen in burns as high as 400°C (Guerrero et al., 2005). Previous studies have suggested that the increase in DOC in burned soil samples is attributed to soluble organic compounds derived from the lysis of microbial cells at such temperature (Serrasolsas and Khanna, 1995; Santos et al., 2016). Many of these microbial derived organic compounds can include oxygenated (such as carbohydrates and proteins) and aliphatic groups. These microbial derived organic compounds may explain the decrease in $SUVA_{254}$ (aromaticity) in the burned treatments of the soil samples. This is consistent with previous studies that showed that $SUVA_{254}$ decreased when soils were burned between 150°C and 250°C (Santos et al., 2016). Generally, the existence of aromatic compounds in burned soil samples comes from enrichment of existing aromatic compounds or formation of new aromatic compounds from the thermal decomposition

of existing organic matter. However, this generally occurs when soils are burned at above 300°C (González-Pérez et al., 2004). As there is probably little to no addition of aromatic compounds into the dissolved state of the OC, the addition of fresh, labile, microbial derived organic compounds diluted the pre-existing aromatic component of DOC and thus causing a decrease in $SUVA_{254}$.

The average molecular size of the DOC in the leachate did not significantly differ from the UB control samples. This result differed from a previous study in which DOC from soils heated to 150°C and 250°C significantly increased average molecular size (i.e. higher $A_{250}:A_{365}$) (Santos et al., 2016). In their study, they suggested that heating samples at those temperatures resulted in small-size molecules undergoing polymerization reactions that resulted in larger molecules. It is also possible that smaller molecular size DOC are preferentially lost when heated between those temperature, resulting in a pool of carbon enriched with higher molecular size compounds. However, in that study the soil samples were heated at the maximum temperature for 1 hour, whereas we heated our samples at the maximum temperature for 30 min. Such thermal degradation and/or polymerization of DOC may be time duration dependent, or even moisture dependent as shown by the increase in average molecular weight of DOC in the SB and RB treatment of the shrubland soil. However, the differences in average molecular weight of the SB and RB treatment were not statistically different than the UB control treatment. Since the average molecular weight does not differ amongst the treatments, it can be inferred that the DOC diffuse within the soil pore water at relatively the same rate assuming that pore sizes and geometry remain the same. Diffusion and/or physical accessibility of organic substrate to

microorganisms is an important factor in decomposition of the substrate as many microbial processes require water (Balesdent et al., 2000).

In review, both the forest and shrubland soils had higher DOC concentration for all three burn treatments when compared to the UB control treatment. The increase in DOC is likely from biodegradable cytoplasmic organic compounds from the lysis of microbial cells. Moreover, the average molecular weight of the DOC in the burned treatments do not differ from each other nor the UB treatment, therefore the DOC should diffuse at relatively the same rate to microbes for decomposition. These observations indicate that the burned treatments should have higher decomposition and respiration of CO₂ over a course of an incubation experiment since there is more DOC to decompose.

3.4.2 CO₂ measurements in forest soil

For both the forest soil with aggregate sizes 0.25-1mm and 1-2mm, the total respiration of C for the DRB and SB treatment did not significantly differ from the UB treatment for the respective sizes (Figures 4 and 6), even though both of those treatments were shown to have significantly higher amounts of DOC in the 2-4 mm sized aggregates. The only treatment to have significantly higher total respiration of C was the RB treatment. This is likely linked to the microscopic breakdown of the soil aggregates from the stress induced by the rapid vaporization of soil pore water as proposed by Albalasmeh et al (2013) and in chapter 2 of this thesis. Aggregated soils are known to have higher tortuosity (Horn and Smucker, 2005) and more complex soil pore geometries that limit diffusion pathways for microbes to have access to organic

carbon for respiration (Scow and Alexander, 1992; Balesdent et al., 2000). The degradation of soil aggregation by rapidly vaporized soil pore water from the low intensity burn likely contributed to the decrease in tortuosity and complex soil pore geometries within the RB treatment of forest soil. This likely allowed the soil microbes to have easier access to the DOC within the soil aggregates.

This is also evident as the RB treatments took a considerable amount of time (t_2 of 21.1 ± 2.4 and 19.9 ± 1.8 days for soil aggregates of size 0.25-1 mm, and 1-2 mm, respectively) until a second pool of carbon appeared. Initially, the rapidly vaporized water slightly weakened the soil aggregate but did not fully break up the soil aggregate to expose physically protected OC. After some time, the soil aggregate break and weaken more to expose the previously physically protected OC. This is consistent with the long-term study made on the soil structure of a shrubland in the eastern Great Basin in Nevada after a controlled, low intensity burn was conducted in August 2009 (Chief et al., 2012; Kavouras et al., 2012). Five days after the burn, the soil structure degraded slightly from a moderate subangular blocky structure to coarse weak subangular blocky structure. After around 9 months, the soil structure broke down further to a structureless soil. In another long-term study, the aggregate stability of forest soils from northeastern Spain that experienced a low intensity burn was shown to increase immediately after the burn (Úbeda and Bernia, 2005). This was attributed to desiccation of inorganic cementing agents. However, after eight months the aggregate stability decreased significantly when compared to unburned soil. Both of these study sites, and also this study, highlight the importance of how the degradation of soil aggregates by rapidly vaporized soil pore water during low intensity burns can take considerable amount of time. The SB treatment

also appears to have a second pool of carbon appear after some time t_2 (4.7 ± 0.7 and 4.2 ± 1.0 days for soil aggregates of size 0.25-1 mm, and 1-2 mm, respectively). However, C_I 's (in Eq. 4 and 6) for the SB treatment was minimal, and it is assumed that initial mineralization of soil C was low due to the SB treatment being burned in the oven for a total of 80 minutes and more of the soil microbes died out, since soil microbes have been known to die when exposed to temperatures of 50-120° C (Hernández et al., 1997; Neary et al., 1999). This is evident as the SB treatment had slightly higher DOC content than the DRB and the RB treatments.

The first order decay constant (k) across all treatments was relatively unchanged when compared to the UB control treatment. However, k was slightly lower in the RB treatments, which meant that the OC in the RB treatments decay at a slower rate. This is probably due to the pool of C being accessed to decomposition in the RB treatment being mostly particulate OC (POC). POC is generally the form of OC that is occluded within soil aggregates, and are known to be less labile and decomposable than free and loose organic matter (Christensen, 2001). This further highlights that the soil aggregates are degrading for the RB treatment, since the soil decomposers in the RB treatment are able to access the pool of C within the soil aggregates that the soil decomposers in the other treatments are not able to access.

3.4.3 CO₂ measurements in shrubland soil

For the shrubland soil with aggregate size 0.25-1mm, the total respiration of C generally increased with burning of the soil aggregates, although the DRB treatment did not significantly differ from the UB treatment (Figure 3-5 and Figure 3-6). Upon closer

look at the total C respiration for this aggregate size (Figure 3-6c) and the leached DOC for the shrubland soil (Figure 3-1b), it appears that they both follow a similar trend for the respective treatments. This is more apparent when plotting the ratio of C_0 to the total carbon pool (C_a) within the soil aggregates vs the ratio of DOC to total organic carbon (TOC) within the soil aggregates (Figure 3-9). The linear increasing trend of respired C to leached DOC is only evident in the shrubland soil aggregates of size 0.25-1mm. This potentially indicates that the increased carbon that is mineralized in the burned shrubland soil aggregates of size 0.25-1 mm is from mineralization of leached microbial lysis, and that it is not particularly from microbial access to physically protected OC within the aggregates, as seen for the forest aggregates.

For the shrubland soil with aggregate size 1-2 mm, there were no differences in total respiration of C across all the treatments. One possible explanation for no difference in respiration could be that the total amount of organic carbon was very small. The TOC content in the shrubland aggregates of 1-2 mm in size is $0.70 \pm 0.01\%$, whereas the TOC content for the forest aggregates of size 0.25-1 mm and 1-2 mm, and the shrubland aggregates of size 0.25-1 mm are $5.73 \pm 0.07\%$, $4.67 \pm 0.09\%$, and $1.25 \pm 0.02\%$, respectively (Table 3-1). Since the shrubland aggregates of size 1-2mm had such low amount of OC, the addition of DOC in the form of microbial lysis may not have contributed too much to additional respiration.

Figure 3-9 indicates that the percentage of biologically available C in the forest aggregates is about an order of magnitude greater than the percentage of biologically available C in the shrubland aggregates, which indicates that there is very small percentage of OC that able to be decomposed within the shrubland soils. There may be

some explanation as to why there is such a low percentage of biologically available carbon in the shrubland soils. Shrubland ecosystems are known to have relatively low net primary productivity in comparison to other ice-free ecosystems (Stiling, 1996). Since there is little fresh input of OC into the soils, most of the available carbon probably has already been mineralized, and the leftover biologically available carbon within the soil aggregates decomposed very quickly, as indicated with the very high k values for the shrubland soils (Figure 3-8). The shrubland soil also has relatively high clay content (Table 3 – 1) The little amount of OC within the shrubland soil is likely chemically stabilized by association with clay minerals, where the OC is mostly sorbed onto the high specific surface area minerals (Mikutta et al., 2006; Schmidt et al., 2011).

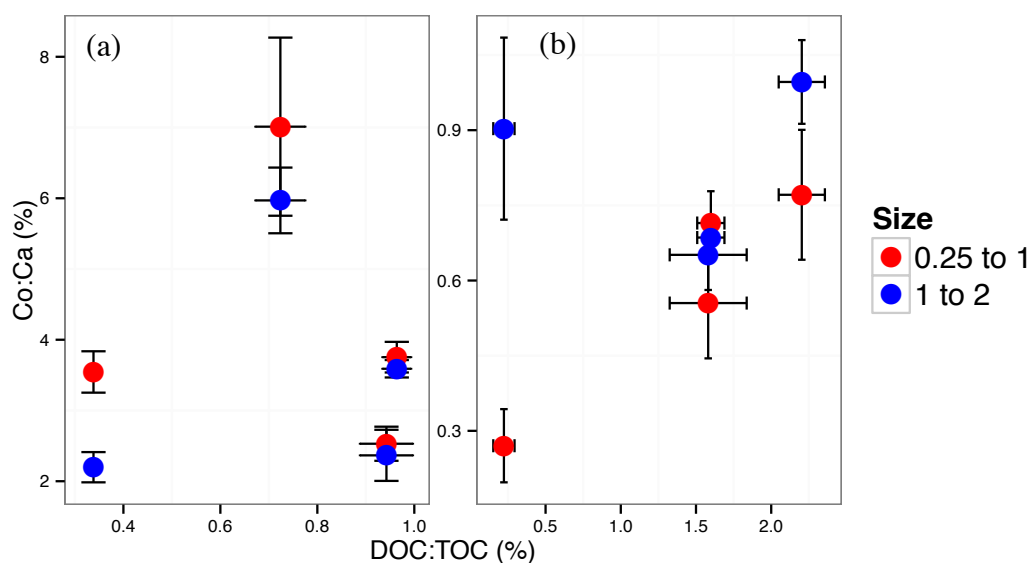


Figure 3-9 Ratio of DOC:TOC vs ratio of C₀:C_a for (a) forest soil and (b) shrubland soil for the two aggregate sizes, where C₀:C_a represents the ratio of the biologically available carbon pool to the total carbon pool (C_a), and DOC:TOC represents the ratio of dissolved organic carbon leached to the total organic carbon.

3.5 Conclusion

This study highlights the important effect that low intensity burn may have on carbon mineralization rate on soil aggregates from two distinct ecosystems. We showed that for a forest soil with high degree of aggregation, low intensity burns can rapidly vaporize soil water which can induce stress onto soil aggregates that cause soil disaggregation over time. This leads to liberation of previously, physically protected soil organic carbon, thus increasing the amount of carbon mineralized. We also showed that for a shrubland soil with low degree of aggregation and organic carbon content, low intensity burns can induce microbial lysis. The lysis of microbes can release biodegradable cytoplasmic organic compounds, which can also increase carbon mineralization in the shrubland soil. Results from both of these distinct ecosystems highlight the importance of low intensity fires and their effects on soil aggregation, in which most previous studies have widely ignored since low intensity fires are presumed to have little effects. Furthermore, these results warrant further investigations of these types of fires onto soil properties, as low intensity burns constitute the majority of fires in the United States and there are limited numbers of studies on these types of fires on soil aggregation.

Chapter 4

Summary and Conclusion

Soil aggregation is one of the most important soil qualities as it has significant control over many physical, chemical, and biological processes in both natural and anthropogenically-altered soils. In fire-prone ecosystems, fire is one of the main agents of soil aggregate degradation. Most studies on fires and their effects on soil aggregation have focused on the effects of medium-to-high intensity burns ($> 220^{\circ}\text{C}$) since organic and inorganic binding agents responsible for soil aggregate are unstable at such temperatures. Meanwhile, limited studies have focused on low intensity fires since they are generally considered benign to soil aggregation. We recently hypothesized that low intensity fires can have a different mechanism of aggregate degradation by rapidly vaporizing soil pore water that can induce stress onto soil aggregates and cause microscopic breakdown that lead to degradation over periods of time (Albalasmeh et al., 2013). This thesis further explored this mechanism of soil aggregate degradation in two ways:

1. Confirming the hypothesized mechanism of soil aggregate degradation by directly measuring the pneumatic pore pressure increase during low intensity burns from two distinct soil types in Chapter 2.
2. Addressing how such mechanism of soil aggregate degradation can affect soil organic carbon decomposition in Chapter 3.

In Chapter 2, we directly measured the pressure rise in soil aggregates wetted to various water contents during low intensity burns. The experimental results showed that wetter soil aggregates exhibited the maximum pneumatic pressure rise from vaporization of soil pore water. Moreover, the tensile strength of soil aggregates decreased with increase in soil water content, suggesting that initially moist soil aggregates are indeed more susceptible to degradation by the proposed mechanism of aggregate degradation. We also developed a model to provide a semi-quantitative indication of the degree of deformation caused by the pore pressure rise within the soil aggregates. We found that the degree of deformation caused by the pneumatic pore pressure increased with increase in initial soil water content. Lastly, we showed that there was no difference in soil organic carbon content between unburned and burned samples (Appendix B), which confirms that degradation of soil aggregates by low intensity fire cannot be explained by loss of soil organic matter content.

The findings from Alabalasmeh et al (2013) and Chapter 2 lead us to investigate how degradation of soil aggregates by soil pore pressure rise can lead to changes in soil biogeochemical processes for the two soil types that were studied in Chapter 2. Specifically, we investigated how such degradation can affect soil organic carbon decomposition. The results presented in Chapter 3 indicates that rapid vaporization of pore water during low intensity burns can lead to higher soil organic carbon decomposition rates in forest soil aggregates since degradation of soil aggregates expose previously physically protected organic carbon to soil microorganisms. In shrubland soil aggregates that have low degree of soil aggregation and soil organic carbon content, it

was shown that low intensity burns can lead to higher rates of decomposition due to lysis of microbial cells that introduced fresh organic compounds into the soil system.

This thesis addressed two important points on low intensity fires and soil aggregation. (1) Low intensity burns can potentially degrade soil aggregates with rapid vaporization of soil pore water. This mechanism is different than medium and high intensity burns since those burns degrade soil by destabilization of soil organic and inorganic binding agents. (2) Degradation of soil aggregates during low intensity burns can lead to previously physically protected soil organic carbon within the soil aggregates being vulnerable to decomposition.

The degradation of soil aggregates by such mechanism can potentially lead to alteration of other ecosystem processes as well. The degradation of soil aggregation can potentially lead to decrease in soil porosity and increase in bulk density. The preceding changes in soil properties can also lead to decrease in hydraulic conductivity and infiltration, which in turn can lead to higher rates of erosion. Soil disaggregation can also affect humans as well. For example, the potential higher rate of erosion can affect downstream resources such as water quality and transport of sediment to other landscapes. Moreover, the increased decomposition rates in soils subjected to low intensity burns (addressed in Chapter 3) can further exacerbate the many effects that anthropogenic climate change can have on the human dimension. We conclude this thesis by reiterating that low severity burns account for more than half of the areas burned in the US from 1984 to 2014 (MTBS, 2017) and that presently there are only a few long-term studies on the effects of the effects of low intensity fires on soil aggregation. Therefore,

there is extensive research that needs to be conducted to develop a database on the effects of low intensity fires on soil alteration in different ecosystems.

References

- Albalasmeh, A.A., M. Berli, D.S. Shafer, and T.A. Ghezzehei. 2013. Degradation of moist soil aggregates by rapid temperature rise under low intensity fire. *Plant Soil* 362(1–2): 335–344.
- AOAC. 1997. Microchemical determination of carbon, hydrogen, and nitrogen, automated method. p. 5–6. *In* Official methods of analysis of AOAC international. 16th ed. AOAC International, Arlington, VA.
- Araya, S.N., M.L. Fogel, and A.A. Berhe. 2017. Thermal alteration of soil organic matter properties : a systematic study to infer response of Sierra Nevada climosequence soils to forest fires. (3): 31–44.
- Arcenegui, V., J. Mataix-Solera, C. Guerrero, R. Zornoza, J. Mataix-Beneyto, and F. García-Orenes. 2008. Immediate effects of wildfires on water repellency and aggregate stability in Mediterranean calcareous soils. *Catena* 74(3): 219–226 Available at <http://linkinghub.elsevier.com/retrieve/pii/S0341816208000040>.
- Bachmann, J., G. Guggenberger, T. Baumgartl, R.H. Ellerbrock, E. Urbanek, M.O. Goebel, K. Kaiser, R. Horn, and W.R. Fischer. 2008. Physical carbon-sequestration mechanisms under special consideration of soil wettability. *J. Plant Nutr. Soil Sci.* 171(1): 14–26.
- Balesdent, J., C. Chenu, and M. Balabane. 2000. Relationship of soil organic matter dynamics to physical protection and tillage. *Soil Tillage Res.* 53(3–4): 215–230.
- Barre, P., and P.D. Hallett. 2009. Rheological stabilization of wet soils by model root and

- fungal exudates depends on clay mineralogy. *Eur. J. Soil Sci.* 60(4): 525–538.
- Benavides-Solorio, J., and L.H. MacDonald. 2001. Post-fire runoff and erosion from simulated rainfall on small plots, Colorado Front Range. *Hydrol. Process.* 15(15): 2931–2952.
- Benavides-Solorio, J.D.D., and L.H. MacDonald. 2005. Measurement and prediction of post-fire erosion at the hillslope scale, Colorado Front Range. *Int. J. Wildl. Fire* 14(4): 457–474.
- Bronick, C.J., and R. Lal. 2005. Soil structure and management: A review. *Geoderma* 124(1–2): 3–22.
- Carroll, E.M., W.W. Miller, D.W. Johnson, L. Saito, R.G. Qualls, and R.F. Walker. 2007. Spatial analysis of a large magnitude erosion event following a Sierran wildfire. *J. Environ. Qual.* 36(4): 1105–1111 Available at <http://www.ncbi.nlm.nih.gov/pubmed/17526890>.
- Carter, M.C., and C.D. Foster. 2004. Prescribed burning and productivity in southern pine forests: A review. *For. Ecol. Manage.* 191(1–3): 93–109.
- Causarano, H. 1993. Factors affecting the tensile strength of soil aggregates. *Soil Tillage Res.* 28: 15–25.
- Certini, G. 2005. Effects of fire on properties of forest soils: a review. *Oecologia* 143(1): 1–10 Available at <http://link.springer.com/10.1007/s00442-004-1788-8>.
- Chenu, C., and A.T. Plante. 2006. Clay-sized organo-mineral complexes in a cultivation chronosequence: Revisiting the concept of the “primary organo-mineral complex.” *Eur. J. Soil Sci.* 57(4): 596–607.
- Chief, K., M.H. Young, and D.S. Shafer. 2012. Changes in Soil Structure and Hydraulic

- Properties in a Wooded-Shrubland Ecosystem following a Prescribed Fire. *Soil Sci. Soc. Am. J.* 76: 1965–1977.
- Choromanska, U., and T.H. DeLuca. 2002. Microbial activity and nitrogen mineralization in forest mineral soils following heating: Evaluation of post-fire effects. *Soil Biol. Biochem.* 34(2): 263–271.
- Christensen, B.T. 2001. Physical fractionation of soil and structural and functional complexity in organic matter turnover. *Eur. J. Soil Sci.* 52(3): 345–353.
- DeBano, L.F. 2000. The role of fire and soil heating on water repellency in wildland environments: A review. p. 195–206. *In* *Journal of Hydrology*.
- DeBano, L.F., P.H. Dunn, and C.E. Conrad. 1977. Fire's effects on physical and chemical properties of chaparral soils. p. 65–74 TS–RIS. *In* *Environmental Consequences of Fire and Fuel Management in Mediterranean Ecosystems*.
- Dexter, A.R., and B. Kroesbergen. 1985. Methodology for Determination of Tensile Strength of Soil Aggregates. *J. agric. Engng Res* 31(August 1983): 139–147.
- Eidenshink, J., B. Schwind, K. Brewer, Z. Zhu, B. Quayle, and S. Howard. 2007. A Project for Monitoring Trends in Burn Severity. *Fire Ecol.* 3(1): 3–21.
- Ekschmitt, K., E. Kandeler, C. Poll, A. Brune, F. Buscot, M. Friedrich, G. Gleixner, A. Hartmann, M. Kästner, S. Marhan, A. Miltner, S. Scheu, and V. Wolters. 2008. Soil-carbon preservation through habitat constraints and biological limitations on decomposer activity. *J. Plant Nutr. Soil Sci.* 171(1): 27–35.
- Flessa, H., W. Amelung, M. Helfrich, G.L.B. Wiesenberger, G. Gleixner, S. Brodowski, J. Rethemeyer, C. Kramer, and P.M. Grootes. 2008. Storage and stability of organic matter and fossil carbon in a Luvisol and Phaeozem with continuous maize

- cropping: A synthesis. *J. Plant Nutr. Soil Sci.* 171(1): 36–51.
- Gaillard, V., C. Chenu, S. Recous, and G. Richard. 1999. Carbon, nitrogen and microbial gradients induced by plant residues decomposing in soil. *Eur. J. Soil Sci.* 50(4): 567–578.
- García-Corona, R., E. Benito, E. de Blas, and M.E. Varela. 2004. Effects of heating on some soil physical properties related to its hydrological behaviour in two north-western Spanish soils. *Int. J. Wildl. Fire* 13(2): 195–199 Available at http://www.publish.csiro.au/view/journals/dsp_journal_fulltext.cfm?nid=114&f=WF03068 (verified 3 December 2015).
- Ghezzehei, T.A. 2004. Constraints for flow regimes on smooth fracture surfaces. 40(March).
- Ghezzehei, T.A. 2012. Soil Structure. p. 1–18. *In Handbook of Soil Science.*
- Ghezzehei, T.A., and D. Or. 2000. Dynamics of soil aggregate coalescence governed by capillary and rheological processes. *Water Resour. Res.* 36(2): 367–379.
- Ghezzehei, T.A., and D. Or. 2001. Rheological Properties of Wet Soils and Clays under Steady and Oscillatory Stresses. (65): 624–637.
- González-Pérez, J.A., F.J. González-Vila, G. Almendros, and H. Knicker. 2004. The effect of fire on soil organic matter - a review. *Environ. Int.* 30(6): 855–870.
- Guerrero, C., J. Mataix-Solera, I. Gómez, F. García-Orenes, and M.M. Jordán. 2005. Microbial recolonization and chemical changes in a soil heated at different temperatures. *Int. J. Wildl. Fire* 14(4): 385–400.
- Guerrero, C., J. Mataix-Solera, J. Navarro-Pedreño, F. García-Orenes, and I. Gómez. 2001. Different Patterns of Aggregate Stability in Burned and Restored Soils. *Arid*

- L. Res. Manag. 15(2): 163–171.
- Harris, D., W.R. Horwáth, and C. van Kessel. 2001. Acid fumigation of soils to remove carbonates prior to total organic carbon or CARBON-13 isotopic analysis. *Soil Sci. Soc. Am. J.* 65(6): 1853.
- Hassink, J., and A. Whitmore. 1997. A model of the physical protection of organic matter in soils. *Soil Sci. Soc. Am. J.* Available at http://www.ncbi.nlm.nih.gov/entrez/query.fcgi?db=pubmed&cmd=Retrieve&dopt=AbstractPlus&list_uids=16286283682683121237&hl=en&num=50related:VW6RkbIABOIJ:scholar.google.com/&hl=en&num=50.
- Hernández, T., C. García, and I. Reinhardt. 1997. Short-term effect of wildfire on the chemical, biochemical and microbiological properties of Mediterranean pine forest soils. *Biol. Fertil. Soils* 25(2): 109–116.
- Heynen, C.E., J.D. Van Elsas, P.J. Kuikman, and J.A. van Veen. 1988. Dynamics of *Rhizobium leguminosarum* biovar *trifolii* introduced into soil; the effect of bentonite clay on predation by protozoa. *Soil Biol. Biochem.* 20(4): 483–488.
- Hillel, D. 1998. *Environmental Soil Physics*. Acad. Press San Diego CA: 771 Available at http://books.google.com/books?id=tP__y5xRd0oC&printsec=frontcover.
- Hoogmoed, W.B., and L. Stroosnijder. 1984. Crust formation on sandy soils in the Sahel I. Rainfall and infiltration. *Soil Tillage Res.* 4(1): 5–23.
- Horn, R., and A. Smucker. 2005. Structure formation and its consequences for gas and water transport in unsaturated arable and forest soils. *Soil Tillage Res.* 82(1): 5–14.
- Jenny, H. 1980. *The Soil Resources, Origin and Behavior*. Springer, New York.
- Jordán, A., L.M. Zavala, J. Mataix-Solera, A.L. Nava, and N. Alanís. 2011. Effect of fire

- severity on water repellency and aggregate stability on Mexican volcanic soils. *Catena* 84(3): 136–147 Available at <http://linkinghub.elsevier.com/retrieve/pii/S0341816210001591>.
- Kavouras, I.G., G. Nikolich, V. Etyemezian, D.W. DuBois, J. King, and D. Shafer. 2012. In situ observations of soil minerals and organic matter in the early phases of prescribed fires. *J. Geophys. Res. Atmos.* 117(D12): n/a-n/a Available at <http://doi.wiley.com/10.1029/2011JD017420>.
- Keeley, J.E. 2009. Fire intensity, fire severity and burn severity: a brief review and suggested usage. *Int. J. Wildl. Fire* 18(1): 116 Available at http://www.publish.csiro.au/view/journals/dsp_journal_fulltext.cfm?nid=114&f=WF07049 (verified 3 December 2015).
- Kleinman, P.J.A., D. Pimentel, and R.B. Bryant. 1995. The ecological sustainability of slash-and-burn agriculture. *Agric. Ecosyst. Environ.* 52(2–3): 235–249.
- Knicker, H. 2007. How does fire affect the nature and stability of soil organic nitrogen and carbon? A review. *Biogeochemistry* 85(1): 91–118.
- Markgraf, W., R. Horn, and S. Peth. 2006. An approach to rheometry in soil mechanics- Structural changes in bentonite, clayey and silty soils. *Soil Tillage Res.* 91(1–2): 1–14.
- Marschner, B., and K. Kalbitz. 2003. Controls of bioavailability and biodegradability of dissolved organic matter in soils. p. 211–235. *In Geoderma*.
- Mataix-Solera, J., a. Cerdà, V. Arcenegui, a. Jordán, and L.M. Zavala. 2011. Fire effects on soil aggregation: A review. *Earth-Science Rev.* 109(1–2): 44–60 Available at <http://dx.doi.org/10.1016/j.earscirev.2011.08.002>.

- Mataix-Solera, J., and S.H. Doerr. 2004. Hydrophobicity and aggregate stability in calcareous topsoils from fire-affected pine forests in southeastern Spain. *Geoderma* 118(1–2): 77–88 Available at <http://www.sciencedirect.com/science/article/B6V67-48V820B-1/2/d112d94f38bfbf80c877883c2aa38928>.
- Mataix-Solera, J., I. Gómez, J. Navarro-Pedreño, C. Guerrero, and R. Moral. 2002. Soil organic matter and aggregates affected by wildfire in a *Pinus halepensis* forest in a Mediterranean environment. *Int. J. Wildl. Fire* 11(2): 107–114 Available at http://www.publish.csiro.au/view/journals/dsp_journal_fulltext.cfm?nid=114&f=WF02020 (verified 3 December 2015).
- Mikutta, R., M. Kleber, M.S. Torn, and R. Jahn. 2006. Stabilization of soil organic matter: Association with minerals or chemical recalcitrance? *Biogeochemistry* 77(1): 25–56.
- Moghaddas, E.E.Y., and S.L. Stephens. 2007. Thinning, burning, and thin-burn fuel treatment effects on soil properties in a Sierra Nevada mixed-conifer forest. *For. Ecol. Manage.* 250(3): 156–166.
- MTBS. 2017. Monitoring Trends in Burn Severity. Available at <http://www.mtbs.gov/>.
- Munkholm, L.J., P. Schjønning, K. Deboz, H.E. Jensen, and B.T. Christensen. 2002. Aggregate strength and mechanical behaviour of a sandy loam soil under long-term fertilization treatments. *Eur. J. Soil Sci.* 53(1): 129–137.
- Neary, D.G., C.C. Klopatek, L.F. DeBano, and P.F. Ffolliott. 1999. Fire effects on belowground sustainability: A review and synthesis. p. 51–71. *In* *Forest Ecology and Management*.
- O’Dea, M.E. 2007. Fungal mitigation of soil erosion following burning in a semi-arid

- Arizona savanna. *Geoderma* 138(1–2): 79–85.
- Piccolo, A., and J.S.C. Mbagwu. 1999. Role of Hydrophobic Components of Soil Organic Matter in Soil Aggregate Stability. *Water* 1810(June 1998): 1801–1810 Available at <http://patriot.net/~tam/humate/mbagwu-piccolo-hydrophobic.pdf>.
- Poesen, J., and J. Savat. 1981. Detachment and transportation of loose sediments by rainfall splash. *Catena* 8(1): 19–41.
- Rutherford, P.M., and N.G. Juma. 1992. Influence of texture on habitable pore space and bacterial-protozoan populations in soil. *Biol. Fertil. Soils* 12(4): 221–227.
- Santos, F., D. Russell, and A.A. Berhe. 2016. Thermal alteration of water extractable organic matter in climosequence soils from the Sierra Nevada, California. *J. Geophys. Res. Biogeosciences*: 1–9 Available at <http://doi.wiley.com/10.1002/2016JG003597>.
- Scharenbroch, B.C., B. Nix, K.A. Jacobs, and M.L. Bowles. 2012. Two decades of low-severity prescribed fire increases soil nutrient availability in a Midwestern, USA oak (*Quercus*) forest. *Geoderma* 183–184: 80–91.
- Schmidt, M.W.I., M.S. Torn, S. Abiven, T. Dittmar, G. Guggenberger, I. a. Janssens, M. Kleber, I. Kögel-Knabner, J. Lehmann, D. a. C. Manning, P. Nannipieri, D.P. Rasse, S. Weiner, and S.E. Trumbore. 2011. Persistence of soil organic matter as an ecosystem property. *Nature* 478(7367): 49–56.
- Scott, V.H., and R.H. Burgy. 1956. Effects of heat and brush burning on the physical properties of certain upland soils that influence infiltration. *Soil Sci. Soc. Am. J.* 82(1): 63–70 Available at <http://www.scopus.com/inward/record.url?eid=2-s2.0-0343837935&partnerID=tZOtx3y1>.

- Scow, K.M., and M. Alexander. 1992. Effect of Diffusion on the Kinetics of Biodegradation: Experimental Results with Synthetic Aggregates. *Soil Sci. Soc. Am. J.* 56: 128–134.
- Serrasolsas, I., and P.K. Khanna. 1995. Changes in heated and autoclaved forest soils of S.E. Australia. I. Carbon and nitrogen. *Biogeochemistry* 29(1): 3–24.
- Stiling, P. 1996. *Ecology: Theories and Applications*. Pentice Hall.
- Stoof, C.R., J.G. Wesseling, and C.J. Ritsema. 2010. Effects of fire and ash on soil water retention. *Geoderma* 159(3–4): 276–285.
- Swanson, F.J. 1981. Fire and geomorphic processes. *Fire regimes Ecosyst. Prop.*: 401–420.
- Úbeda, X., and S. Bernia. 2005. The effect of wildfire intensity on soil aggregate stability in the Cadiretes Massif , NE Spain. (May 2004): 37–45.
- Urbanek, E. 2013. Why are aggregates destroyed in low intensity fire? *Plant Soil* 362(1–2): 33–36.
- USDA. 2012. *Introduction to Prescribed Fire in Southern Ecosystems*. South. Resesarch Stn. (August).
- Zavala, L.M., A.J.P. Granged, A. Jordán, and G. Bárcenas-Moreno. 2010. Effect of burning temperature on water repellency and aggregate stability in forest soils under laboratory conditions. *Geoderma* 158(3–4): 366–374 Available at <http://linkinghub.elsevier.com/retrieve/pii/S0016706110001953>.

Appendix A

Measuring soil moisture evaporation rate during heating treatments

The following section provides supplementary information for measuring soil moisture evaporation rate of the soil aggregates during the heating treatments in Chapter 2. Soil aggregates were wetted to the selected matric potentials by placing them on porous plates inside a pressure plate apparatus (Soilmoisture Equipment Corp pressure plate extractor). The soil aggregates were lightly sprayed by a fine mist of water prior to being gradually wetted by capillary action. The aggregates were equilibrated at the desired matric potential level for 24 hours.

The soil aggregates were then placed on a mass scale and were heated with a heat gun (Milwaukee heat gun model 1400) for 15 minutes at temperatures around 175°C that corresponds to typical temperatures found in low intensity burns. The mass of the soil aggregate was continuously measured throughout the heating experiment. 13 forest aggregates and 14 shrubland aggregates were used for this experiment.

The mass of the soil aggregate throughout the heating experiment was converted to the gravimetric water content, and was modeled to decrease exponentially with time

$$\omega = \omega_0 e^{-kt} \quad (\text{Eq. A.1})$$

where ω is the gravimetric water content, ω_0 is the initial gravimetric water content, and k is the first order decay constant.

An example plot of the measured gravimetric water content of the soil aggregates during the heating experiment and the model fit are shown in Figure A-1. The average k for the forest and shrubland aggregates were $3.76 \times 10^{-3} \text{ s}^{-1} \pm 1.12 \times 10^{-3} \text{ s}^{-1}$ (mean \pm standard deviation) for the forest soil, and $5.18 \times 10^{-3} \text{ s}^{-1}$ to $9.31 \times 10^{-4} \text{ s}^{-1}$, respectively.

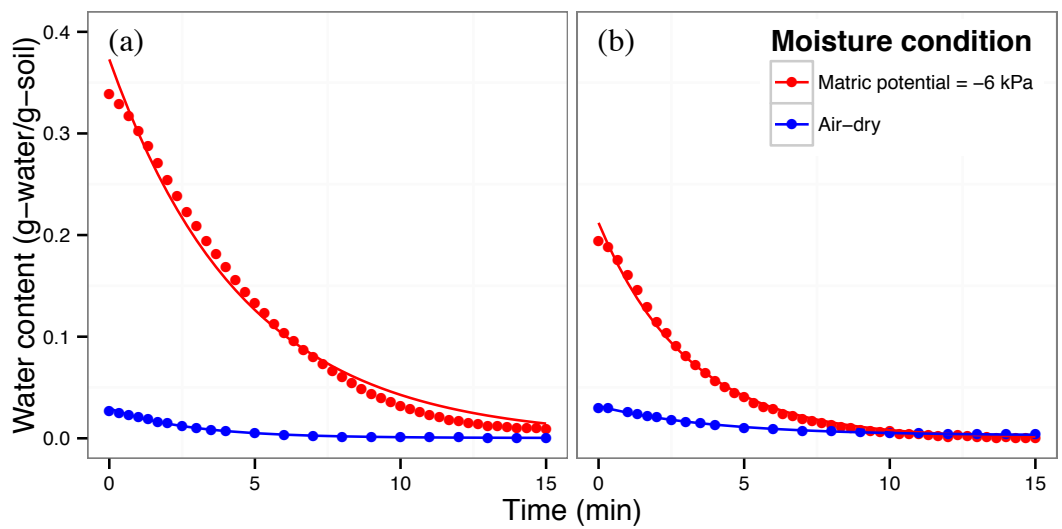


Figure A-1 Example plots of the gravimetric water content of the soil aggregates during a heating experiment and the model fit for air-dried soil aggregates and soil aggregates at -6 kPa matric potential for the (a) forest and (b) shrubland soil. Air-dried matric potentials for the forest and shrubland soil are -94,230 kPa and -123,603 kPa, respectively

Appendix B

Energy partitioning calculation

The following sections provide supplementary information for the aggregates used in Chapter 2. The goal of this section is to calculate where the energy during the heating experiment goes and in the end show that most of the energy goes into vaporizing soil moisture. The amount of energy that the soil aggregate took up per unit mass of soil during the duration of the heating experiment can be given by

$$E_{total} = E_{H_2O} + E_{soil} + E_{blk} + E_{vap} \text{ (Eq. B.1)}$$

where E_{H_2O} is the energy required to heat the total amount of water in the soil aggregate from 25°C to 100°C, E_{soil} is the energy required to heat mineral portion of the soil from 25°C to the maximum temperature observed, E_{blk} is the black body radiant emittance given as a function of the soil surface temperature, and E_{vap} is the total energy required to vaporize the water in the soil aggregate.

B.1 Calculating E_{H_2O} and E_{vap}

The amount of energy required to heat and vaporize the total amount of water in the soil aggregate per unit mass of soil can be determined from the gravimetric water content (μ). The gravimetric water content of the soil aggregates at the selected matric potentials were determined by wetting soil aggregates to the selected matric potentials by

placing them on porous plates inside a pressure plate apparatus. The forest aggregates were then gradually wetted by capillary action from a thin film of water on top of the porous plates. The shrubland aggregates were lightly sprayed by a fine mist of water prior to being gradually wetted by capillary action. The aggregates were equilibrated at the desired matric potential level for 24 hours. Afterwards, they were removed from the plate and the gravimetric water content was determined by drying them in an oven at 105°C for 24 hours.

E_{H_2O} was then determined by

$$E_{H_2O} = C_{H_2O}T\mu \quad (\text{Eq. B.2})$$

where C_{H_2O} is the specific heat capacity of water (4.184 J g⁻¹ °C⁻¹), and T is equal to 75°C, the difference between 100°C and 25°C, the assumed starting temperature before the heating experiment. E_{vap} was then determined by

$$E_{vap} = Q\mu \quad (\text{Eq. B.3})$$

where Q is the latent heat of vaporization of water (2264.76 J g⁻¹).

B.2 Calculating E_{soil}

The amount of energy required to heat the solid soil mass within each of the soil aggregates can be determined from the maximum observed soil surface temperature. The maximum observed soil surface temperature was determined by an infrared thermometer (Omega infrared thermometer OS1327D), and then \square_{soil} was determined by

$$E_{soil} = C_S(T_{max} - 25^\circ\text{C}) \quad (\text{Eq. B.4})$$

where C_S is the specific heat capacity of the solid soil mass ($0.8 \text{ J g}^{-1} \text{ }^\circ\text{C}^{-1}$), and T_{max} is the maximum observed soil surface temperature. A difference of 25°C was taken because this was assumed to be the starting temperature before the heating experiment.

B.3 Calculating E_{blk}

E_{blk} is defined as the energy radiating out of the soil aggregates in terms of the temperature. Because it was difficult to determine the bulk density of large soil aggregates, we assumed the bulk density (ρ_b) of all the soil aggregates were 1.5 g cm^{-3} and also assumed the soil aggregates were a perfect spherical shape. Thus, the surface area of the soil aggregates were determined by

$$A = \pi^{1/3}(6V)^{2/3} \text{ (Eq. B.5)}$$

where V is the volume of the spherical soil aggregate, determined by

$$V = \frac{\rho_b}{m} \text{ (Eq. B.6)}$$

where m is the mass of the soil aggregate.

The power radiating out of the soil aggregate can be determined by Stefan-Boltzmann law

$$j^* = \varepsilon\sigma T^4 \text{ (Eq. B.7)}$$

where ε is the emissivity (0.92), σ is the Stefan-Boltzmann constant ($5.67 \times 10^{-8} \text{ W m}^{-2} \text{ K}^{-4}$), and T is the soil aggregate surface temperature at each time step determined as determined by an infrared thermometer (Figure 2-1).

E_{blk} is then determined by

$$E_{blk} = \int_0^\tau \frac{j^* A}{m} dt \text{ (Eq. B.8)}$$

where τ is the duration of the heating experiment.

B.4 Results and discussion of energy partitioning calculation

The calculated energy partitioning is shown in Table B-1. For both of the soil types, some of the energy during the heating experiment went into heating the soil moisture and heating the solid soil mass. Most of the energy went into radiating energy and vaporizing the soil moisture. For the forest soils, with the exception of the air-dried treatment (-94,230 kPa matric potential), the majority of the energy went into vaporizing soil moisture. For the desert soils, the majority of the energy did not go into vaporization of soil moisture, but nonetheless it is still a large proportion of the energy.

Table B-1 Summary of the energy partitioning calculation for forest and shrubland soil aggregates at various water contents during the heating experiment. For the moist soil aggregates, a large proportion of the energy went into vaporization of the soil moisture

Soil	Matric potential (-kPa)	Water content (g/g)	E_{H_2O} (J/g)	E_{soil} (J/g)	E_{blk} (J/g)	E_{vap} (J/g)	$E_{vap}:E_{total}$
Forest	6	0.413±0.004	129.599	117.049	337.867	935.346	0.615
	10	0.359±0.007	112.654	110.412	317.950	813.049	0.600
	30	0.336±0.018	105.437	118.435	344.838	760.959	0.572
	100	0.311±0.011	97.592	123.705	373.640	704.340	0.542
	94230	0.021±0.000	6.590	122.288	449.107	47.560	0.076
Shrubland	6	0.195±0.002	61.191	127.615	431.043	441.628	0.416
	10	0.180±0.005	56.484	130.326	428.047	407.657	0.399
	20	0.174±0.006	54.601	113.175	360.787	394.068	0.427
	100	0.138±0.006	43.304	132.235	457.550	312.537	0.331
	123603	0.024±0.003	7.5312	117.440	442.720	54.354	0.087

Appendix C

Organic carbon content of large soil aggregates

The following section provides supplementary information for the aggregates used in Chapter 2. Soil aggregate degradation by high intensity fires is often attributed to loss of soil organic matter (Mataix-Solera et al., 2011). Therefore, controlled burns are generally managed to be low in intensity to limit the loss of soil organic matter. However, a previous study has shown that soil aggregates can degrade during low intensity burns due to rapid vaporization of soil moisture, even though there is no significant loss in soil organic matter (Albalasmeh et al., 2013). Here, we show that the organic carbon content of the soil aggregates is not significantly different than the unburned samples, which is consistent with previous findings that soils burned at around 175°C do not experience significant changes in soil organic matter content (Araya et al., 2017).

Triplicate samples of soil aggregates burned at multiple matric potentials from the heating experiment were selected at random. The samples were ground by mortar and pestle, and sent to the UC Davis Analytical Laboratory to be analyzed for total organic carbon (TOC) content (AOAC, 1997) after removal of carbonates by acid fumigation (Harris et al., 2001). Comparison of burn treatments on TOC content was performed using one-way ANOVA with R statistical software (r-project.org).

TOC content of UB samples is 4.09 ± 0.51 % and 0.36 ± 0.01 % for the forest and shrubland soil aggregates, respectively (Figure B1). The TOC content of the burned samples was not significantly different than the UB samples for both soil types. The results were comparable to previous findings in which soil organic matter content is found to be relatively stable at burns in such low temperature (Stoof et al., 2010; Zavala et al., 2010; Mataix-Solera et al., 2011).

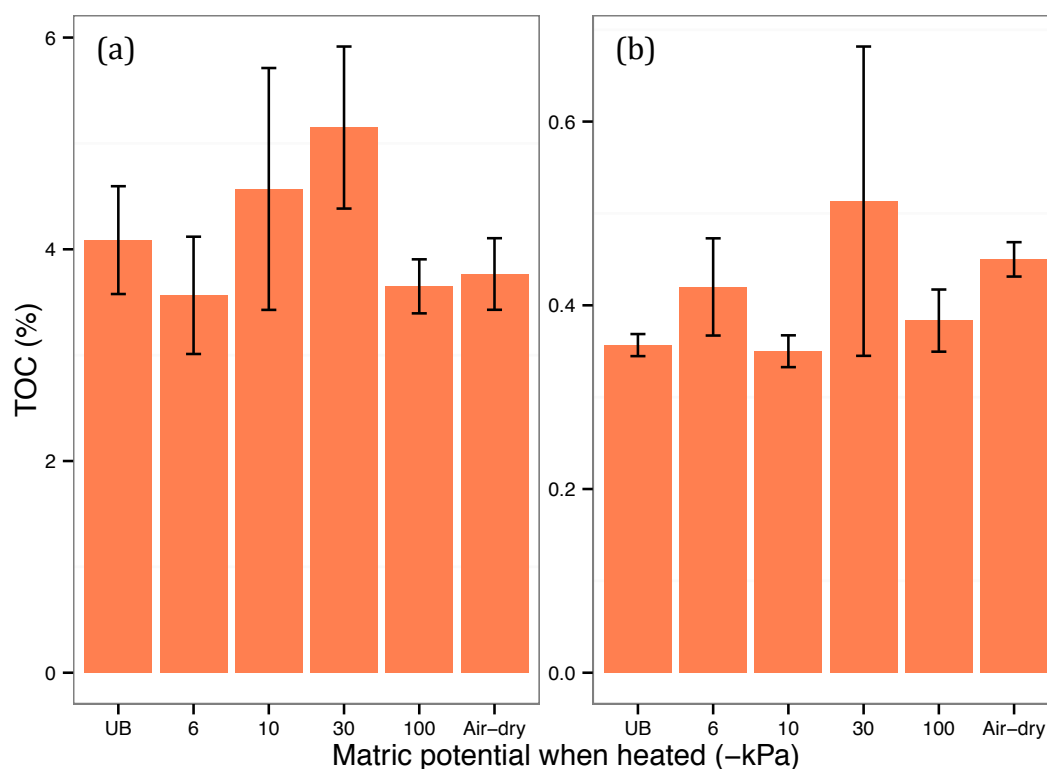


Figure C-1. Total organic carbon (TOC) content of unburned (UB) soil aggregates and selected soil aggregates burned at various matric potentials for (a) forest soil and (b) shrubland soil. There were no significant differences in TOC content between UB soil aggregates and soil aggregates burned at various matric potentials. (mean \pm standard error, where $n = 3$).